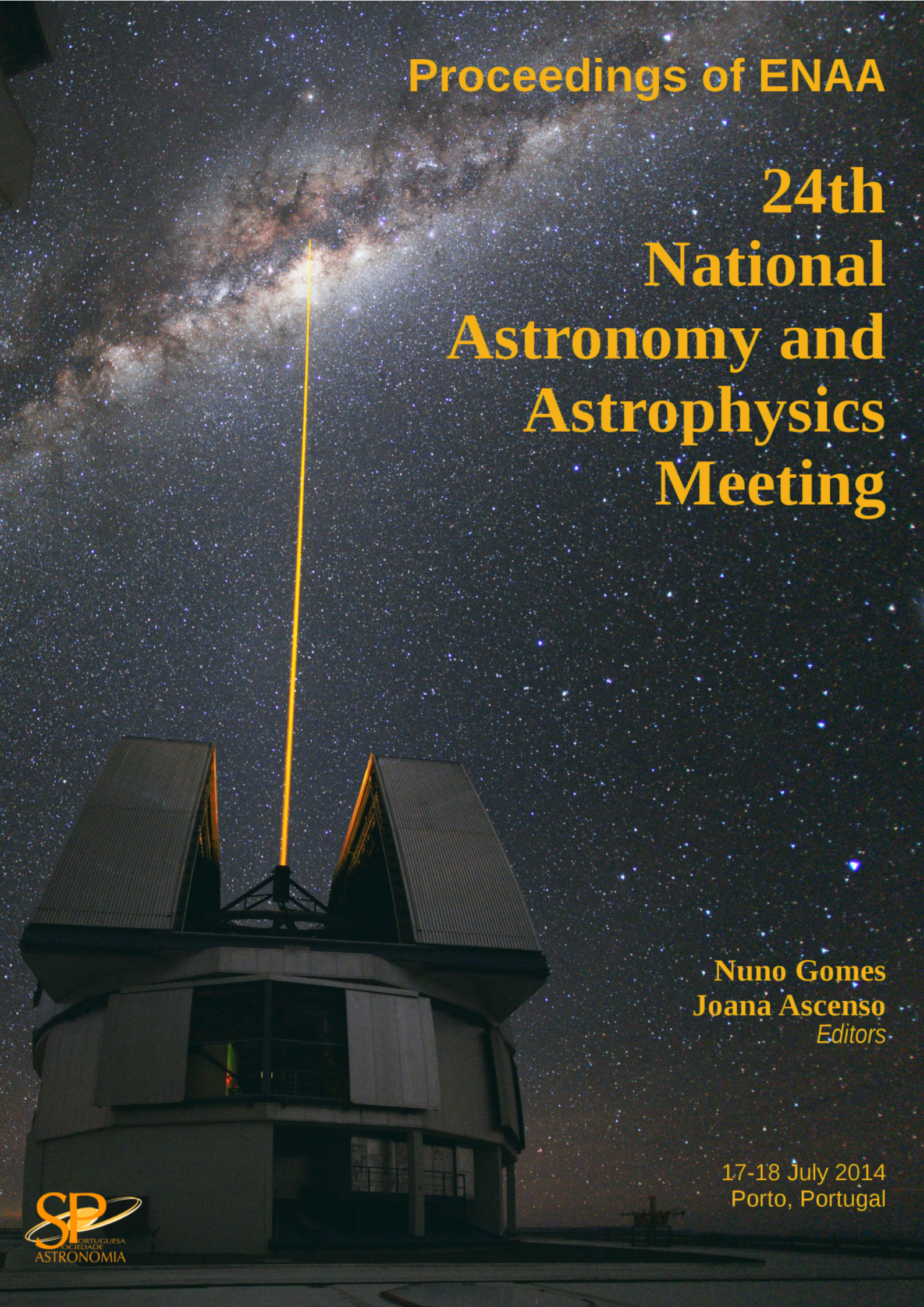

Proceedings of ENAA

24th National Astronomy and Astrophysics Meeting

Nuno Gomes
Joana Ascenso
Editors

17-18 July 2014
Porto, Portugal

SP SOCIEDADE PORTUGUESA ASTRONOMIA

Proceedings of the 24th edition of the

National Astronomy and Astrophysics Meeting

(ENAA XXIV)

Porto, Portugal

Nuno Gomes, University of Porto
Joana Ascenso, University of Porto

17–18 July, 2014

Organised by
Portuguese Astronomical Society (SPA)

Published by
Sociedade Portuguesa de Astronomia
http://www.sp-astronomia.pt/enaa

ISBN: 978-989-99087-1-0

Credits
Cover design: Nuno Gomes & Paulo Garcia
Cover photo: European Southern Observatory / Y. Beletsy
Document prepared in LaTeX, using `confproc` package, version 0.8.

Printed in Porto by Sociedade Portuguesa de Astronomia – August 2014

Supported by

Scientific Organising Committee

Alberto Krone-Martins
André Moitinho de Almeida
Dário Passos
David Sobral
Francisco Lobo
Helena Morais
Joana Ascenso (co-coordinator of the scientific programme)
Jorge Rocha
Mário Santos
Nanda Kumar
Patrícia Gonçalves
Paulo Gordo
Paulo J. V. Garcia (coordinator of the scientific programme)
Pedro Figueira

Local Organising Committee

Narsireddy Anugu
Nuno Gomes (coordinator of the local organisation)
Nelma Alas Silva
Paulo Andrade
Sandra Costa

Prizes Awarding Committee

Alberto Krone-Martins
André Moitinho de Almeida
Dário Passos
David Sobral
Jorge Rocha
Patrícia Gonçalves
Paulo J. V. Garcia
Pedro Figueira

Introduction

The 24^{th} edition of the National Astronomy & Astrophysics Meeting (ENAA) took place at the Faculdade de Engenharia da Universidade do Porto (FEUP), the 17^{th} and 18^{th} July 2014. It was organized by the SIM Laboratory, FCT Unit n. 4006, in collaboration with the Portuguese Astronomy Society.

The meeting presented a panorama of the Portuguese Astronomy & Astrophysics research and development. The contributions were made in the several thematic domains of the International Astronomy Union (as defined in the 28th General Assembly): a) Fundamental Astronomy; b) Facilities, Technologies and Data Science; c)Education, Outreach and Heritage; d) High Energy Phenomena and Fundamental Physics; e) Sun and Heliosphere; f) Planetary Systems and Bioastronomy; g) Stars and Stellar Physics; h) Interstellar Matter and Local Universe; i) Galaxies and Cosmology.

The meeting was also an occasion to strengthen the interactions between the members of the Portuguese Astronomy & Astrophysics community, to the presentation of young researchers' work, to the awarding of prizes, to debate the national science policy for Astronomy & Astrophysics and to present the dimensions of scientific culture, economic impact and innovation and interaction with the society.

This was the first National Astronomy & Astrophysics meeting where double blind refereeing was implemented, each communication being refereed by three SOC members.

During the meeting several prizes were awarded, namely:

- 24th ENAA Outstanding Talk, to Eduardo P. Alves
- 24th ENAA Outstanding Poster, to Narsireddy Anugu
- 24th ENAA Outstanding ESO result, to David Sobral

I take this opportunity to thank the support from the FAC fund of FCT, Porto University and the FEUP Department of Engineering Physics. I warmly thank the LOC for all the work and dedication in preparing such a successful meeting.

Paulo J.V. Garcia, Khongoryn Els, 18^{th} August 2014

CONFERENCE PROGRAMME

Day 1, 17th of July

Oral Session: Highlights in Facilities, Technologies and Data Science

1 *J. Afonso, H. Messias*
The Portuguese ALMA Centre of Expertise – PACE

3 *Carlos J. A. P. Martins*
The COrE+ Proposal: Current Status

5 *Nuno Gomes, Paulo J. V. Garcia, Éric Thébaut*
Best configurations for image reconstruction

7 *Narsireddy Anugu, Paulo J. V. Garcia, António Amorim, Paulo Gordo, Frank Eisenhauer, Jorge Abreu*
Experimental results of an infrared aberration tracking using a correlation algorithm on two star extended field

Poster Session: Facilities, Technologies and Data Science

9 *António Amorim, Paulo J. V. Garcia, Paulo Gordo, Narsireddy Anugu, Jorge Abreu*
Building the GRAVITY instrument for the ESO VLTI

11 *Narsireddy Anugu, Paulo J. V. Garcia, António Amorim, Paulo Gordo, Frank Eisenhauer, Oliver Pfhul, Nicolas Blind, Jorge Abreu*
Measurement of VLT pupil motions using a 2x2 lenslet evaluated aberrations

13 *Narsireddy Anugu, Paulo J. V. Garcia, Ekkehard Wieprecht, António Amorim, Paulo Gordo, Leonard Burtscher, Thomas Ott, Frank Eisenhauer, Jorge Abreu, Nicolas Blind*
Design, development and calibration of the GRAVITY acquisition camera software to monitor four telescope beams

15 *Nuno Gomes, Françoise Delplancke*
Effects of anisoplanatism on the visibility amplitudes and phase variances measured by the PRIMA fringe trackers

17 *Rui Curado da Silva*
A Compact Solar Hard X-ray Polarimeter

Oral Session: Highlights in Cosmology and Fundamental Physics

19 *José Pedro Vieira*
Wiggly cosmic string evolution

21 *Inês Leite, Carlos Martins, José Correia*
Effects of Biases in Domain Wall Network Evolution

23 *Miguel Ferreira, Oriol Frigola, Carlos Martins, Mafalda Monteiro, Joan Solà*
Consistency tests of the stability of fundamental couplings and unification scenarios

25 *Ana Catarina Leite, Carlos Martins, P. Pedrosa*
Fundamental Cosmology from Precision Spectroscopy: Varying Couplings

27 *Eduardo P. Alves, Thomas Grismayer, Ricardo Fonseca, Luís Silva*
Large-scale magnetic field generation via electron-scale instabilities in unmagnetized shear flows

29 *Pedro Leal, Luís Ventura, Carlos Martins*
Fine-structure constant constraints on Bekenstein-type models

Poster Session: Cosmology and Fundamental Physics

31 *Rui Alves, Carlos Martins, Ana Marta Pinho*
Evolution of the fine-structure constant in quintessence-type models

33 *Ana Marta Pinho, Carlos Martins, Rui Alves*
Fine-structure constant constraints on quintessence-type models

35 *Masato Minamitsuji*
Disformal transformation of cosmological perturbations

Day 2, 18th of July

Oral Session: Highlights in Stars and Stellar Physics (including the Sun and Heliosphere)

37 *Dário Passos, Paul Charbonneau*
Latest results from global 3D MHD simulations of solar convection and dynamo action

39 *Ângela Santos, Margarida Cunha, Pedro Avelino*
Empirical solar/stellar cycle simulations

41 *João Faria*
The interesting case of HD41248: stellar activity, no planets?

Poster Session: Stars and Stellar Physics (including the Sun and Heliosphere)

43 *Giancarlo Pace*
A platform for LBL: a key to take properly into account the earth atmosphere transmittance

45 *Ana Brito, Ilídio Lopes*
The upper layers of Alpha-Centauri A: footprint of a new rapid variation layer

47 *Ana Rei, Jorge Gameiro, Sílvia Alencar*
Fundamental stellar parameters determination for WTTS in NGC 2264

Oral Session: Planetary Systems and Bioastronomy

49 *Diana Cunha, N. C. Santos, P. Figueira, A. Santerne, J. L. Bertaux, C. Lovis*
Impact of micro-telluric lines on precise radial velocities

51 *Pedro Figueira*
Lithium depletion of planetary-host stars

53 *Vardan Adibekyan, J. I. González Hernández, E. Delgado Mena, S. G. Sousa, N. C. Santos, G. Israelian, Pedro Figueira, S. Bertran de Lis*
Is there a signature of planet formation in solar analogs?

55 *M. A. Salgueiro da Silva, Cristiana Silva, Teresa Seixas*
The role of single-particle phase function on spectral deconvolution of asteroidal regoliths

Poster Session: Planetary Systems and Bioastronomy

57 *Mahmoudreza Oshagh*
Effect of stellar activity on the high precision transit light curve

Oral Session: Galaxies

59 *David Sobral*
The stellar mass function of star-forming galaxies and the mass-dependent SFR function since z=2.23

61 *Hugo Messias, Bahram Mobasher, José Manuel Afonso*
Hot-dust (690 K) Luminosity Density and Its Evolution in the Last 7.5 Gyr

63 *Andrew Humphrey*
Extreme CII emission in type 2 quasars at z 2.5: a signature of kappa-distributed electron energies?

65 *Leandro Cardoso, Jean Michel Gomes, Polychronis Papaderos*
Evaluating the robustness of state-of-the-art Spectral Synthesis codes when applied to Active Galaxies

Poster Session: Galaxies

67 *Hugo Messias, Rob Ivison, H-Atlas Team*
Herschel-ATLAS and ALMA: HATLASJ142935.3-002836, a major merger at z=1.027?

69 *Pauline Vielzeuf, Carlos Martins*
Evolution of the fine-structure constant in runaway dilaton models

Oral Session: Education, Outreach and Heritage

71 *Cátia Cardoso*
ESERO Portugal

73 *Alexandre Aibéo, Jorge Grave, Manuel Silva*
Olympiads of Astronomy 2014 edition

Selection of photos

And Now for Something Completely Different

75 *Distinguished participants*

85 List of Authors

The Portuguese ALMA Centre of Expertise - PACE

J. Afonso[1,2,3], H. Messias[1,2,3]

[1] *Instituto de Astrofísica e Ciências do Espaço, Universidade de Lisboa, OAL, Tapada da Ajuda, PT1349-018 Lisboa, Portugal*
[2] *Departamento de Física, Faculdade de Ciências, Universidade de Lisboa, Edifício C8, Campo Grande, PT1749-016 Lisbon, Portugal*
[3] *Centro de Astronomia e Astrofísica da Universidade de Lisboa, OAL, Tapada da Ajuda, PT1349-018 Lisboa, Portugal*

Abstract

The Centre for Astronomy and Astrophysics of the Faculty of Sciences of the University of Lisbon (CAAUL) has recently seen its capabilities for ALMA research internationally recognized, being named by ESO as an ALMA Centre of Expertise. This is a result of an objective effort over the last few years to increase the national capability in the exploration of this revolutionary observatory. The Portuguese ALMA Centre of Expertise (PACE) is now ready to provide face-to-face support to the Portuguese community regarding all stages of ALMA observing, from pre-Cycle ALMA promotion and proposal preparation and submission, to data reduction and archival research. PACE is also already actively supporting the ALMA project by participating in the task of ALMA data validation and quality assurance. Here we will describe the responsibilities and capabilities of PACE and show the potential of ALMA in a wide variety of science fields, from our own Sun and Solar System, to galaxy formation and cosmology.

The Atacama Large (sub-)Millimetre Array consortium is composed by three partners (Europe, North-America, and East-Asia) and the host country (Chile). Each of the partners has an ALMA Regional Centre (ARC), which works as a means of closer contact between the local community and the facility. The European ARC is organised distinctively, where "nodes" and "Centers of Expertise" have been created in specific research centres in Europe in addition to the central ARC node, at ESO. Nodes contribute with key expertise improving the user support capability in Europe. Centres of Expertise are aimed at developing key expertise while supporting their local (national) user community in the use of ALMA. While top level responsibilities are still reserved to the central ARC node (such as distribution of calls for proposals or managing the time allocation procedures), others are distributed among the Nodes and Centers of Expertise improving the efficiency of user support (e.g., the speed of data delivery to the PI). The latter include: (i) face-to-face interaction with the community in order to directly support proposal preparation, data reduction, or archival research; (ii) phase II proposal scheduling and execution; (iii) community preparation via meetings and visits to institutes; and (iv) outreach.

As a Centre of Expertise, PACE will hold specific duties. The national community now has access to close support regarding proposal preparation and submission, archival research or just seeking the latest information on ALMA. PACE will continue the task of organising the ALMA National Community Days in preparation for upcoming ALMA Calls for Proposals and performing meetings to promote ALMA and increase its use by the national community. PACE, as a support facility, welcomes visitors at the Astronomical Observatory of Lisbon, where it is located, and where the community will find dedicated personnel and computer hardware. PACE plans to develop

unique expertise among the EU ARC network, thus further improving the ALMA user support capability in Europe.

The COrE+ Proposal: Current Status

C. J. A. P. Martins[1], on behalf of the COrE+ Collaboration

[1] *Centro de Astrofísica, Universidade do Porto, Rua das Estrelas, 4150-762 Porto, Portugal*

Abstract

COrE+ is a proposal for a medium-class mission within the ESA Cosmic Vision program, addressing key scientific questions requiring high sensitivity, full-sky observations of the sky emission at wavelengths in the millimeter and sub-millimeter range. I have described the development and current status of the proposal and gave an overview of the new science that will be made possible by COrE+.

More detailed information may be found at the PRISM Extended White Paper which was published at JCAP 1402 (2014) 006 and is also available from arXiv:1310.1554.

This work was done in the context of the project PTDC/FIS/111725/2009 from FCT (Portugal). C.J.M. is also supported by an FCT Research Professorship, contract reference IF/00064/2012, funded by FCT/MCTES (Portugal) and POPH/FSE (EC).

Best configurations for image reconstruction

Nuno Gomes[1,2], Paulo J. V. Garcia[1], Éric Thiébaut[3]

[1] *Laboratório de Sistemas, Instrumentação e Modelação em Ciências e Tecnologias do Ambiente e do Espaço (SIM)/Faculdade de Engenharia da Universidade do Porto (FEUP), Rua Dr. Roberto Frias, s/n, 4200-465 Porto, Portugal*
[2] *Faculdade de Ciências da Universidade do Porto (FCUP), Rua do Campo Alegre, s/n, 4169-007 Porto, Portugal*
[3] *Université de Lyon, Lyon, F-69003, France; Université Lyon 1, Observatoire de Lyon, 9 avenue Charles André, Saint-Genis Laval, F-69230, France; CNRS, UMR 5574, Centre de Recherche Astrophysique de Lyon ; École Normale Supérieure de Lyon, Lyon, F-69007, France*

Abstract

A new set of instruments capable of measuring the full phase of the visibility — like PRIMA and GRAVITY at ESO, for instance — has reignited the discussion about which phase retrieval technique is the best for interferometric image reconstruction: phase referencing or closure phase. If, on the one hand, under the same observational conditions, phase referencing leads to better image reconstructions than closure phase, specially at lower SNR scenarios[1], because it delivers more phase information, on the other hand, phase referencing instruments usually combine less telescopes during observations than closure phase ones, due to technical constraints, and they need a centre-symmetrical reference close by the scientific source in order to measure the visibility phase. Interferometers thus tend to make available instruments reading the bi-spectrum more easily than instruments providing full phase information. Examples are AMBER, PIONIER and future MATISSE at ESO, MIRC at CHARA, and the forthcoming MROI facility.

An unanswered question in this scenario is which type of instrument should be chosen for a fixed number of nights: a phase referencing like instrument, delivering full phase information but combining less telescopes, or a closure phase like instrument, acquiring less phase data but combining more apertures.

With the aim of answering this question, noisy measurements were generated as if two simulated astronomical objects were mock observed with the VLTI for different configurations and type of instruments. A cluster of stars and a young stellar object (YSO) were observed with ($\dot{a}$) two telescopes using phase referencing (2TPhR, PRIMA + AMBER like) and three telescopes using closures (3TCPh, AMBER like) during 6 nights, ($\dot{b}$) with three telescopes using phase referencing (3TPhR, GRAVITY like) and four telescopes using closures (4TCPh, PIONIER like) during 3 nights, and (c) with four telescopes using phase referencing (4TPhR, GRAVITY like) and 6 telescopes using closures (6TCPh, VSI or MIRC like) during one night.

It was developed a method to estimate the effective PSF for each UV-space coverage before accessing the quality of restored images, and the UV-coverage in the phase referencing case was improved, by uniformly paving the (u, v) plane while keeping the total number of sampled spatial frequencies.

After restoration using the Multi-aperture image Reconstruction Algorithm (MiRA)[3], the images were compared to their original counterparts by means of two quality functions.

For the majority of the configurations, the results point to comparable performances of phase referencing and closure phases, when the UV-space is judiciously chosen.[2]

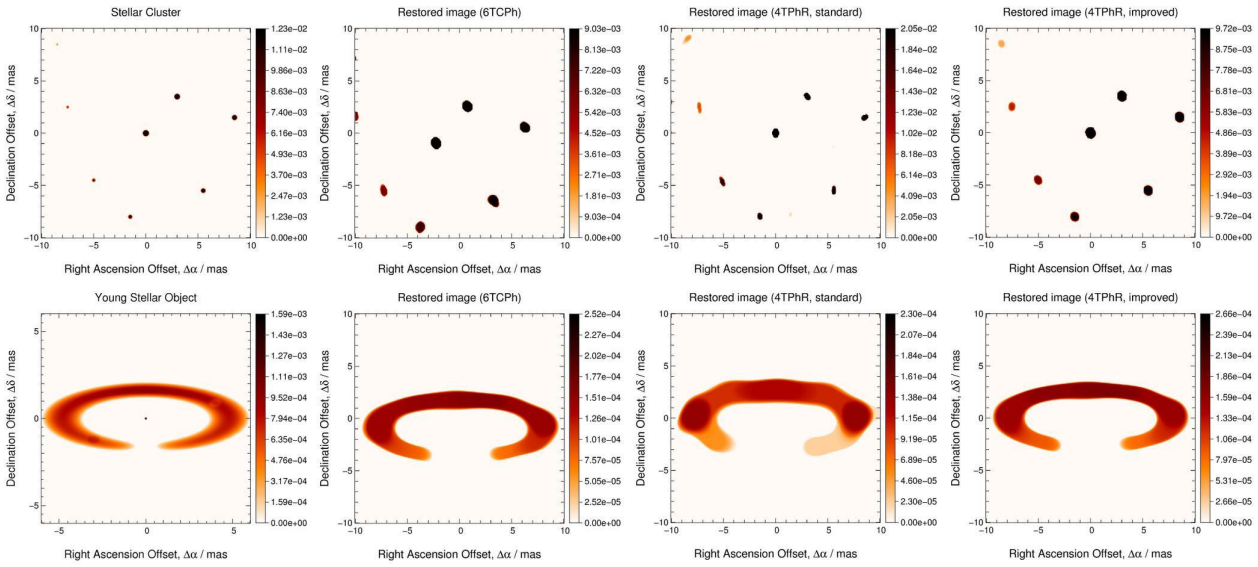

Figure 1: *Top row*: model image of the stellar cluster, restored image in the closure phase (CPh) case, restored image in the phase referencing (PhR) standard UV-coverage case, restored image in the PhR improved UV-coverage case. *Bottom row*: model image of the YSO, restored image for the CPh case, restored image for the PhR standard UV-coverage case, restored image for the PhR improved UV-coverage case.

Acknowledgements

This work was made possible by funding from projects PTDC/CTE-AST/116561/2010, and the European Community's Seventh Framework Programme under Grant Agreement 312430, as well as from Fundação para a Ciência e Tecnologia grant SRFH/BD/44282/2008.

References

[1] Gomes, Nuno; Garcia, Paulo J. V.; Thiébaut, Eric M.; Renard, Stéphanie; Filho, Mercedes, "*Comparison between closure phase and phase referenced interferometric image reconstructions*", SPIE (2010).

[2] Gomes, Nuno; Garcia, Paulo J. V.; Thiébaut, Éric, "*Two, three, four or six telescopes with phase referencing or closure phase relations: the best tactics for interferometric image reconstruction*", SPIE, in press (2014).

[3] Thiébaut, Éric, "*MIRA: an effective imaging algorithm for optical interferometry*", SPIE (2008).

Experimental results for infrared aberration tracking using a correlation algorithm on two star extended field

Narsireddy Anugu[1], Paulo Garcia[2], Antonio Amorim[3], Paulo Gordo[4], Frank Eisenhauer[5], Jorge Abreu[6]

[1] *Universidade do Porto, Faculdade de Engenharia, Laboratório SIM Unidade FCT no 4006, Rua Dr. Roberto Frias, s/n, 4200-465 Porto, Portugal*
[2] *SIM and FCUL - Edificio C8, Campo Grande, P1749016 Lisboa, Portugal*
[3] *Max Planck Institute for extraterrestrial Physics, PO Box 1312, Giessenbachstr., 85741 Garching, Germany*

Abstract

The GRAVITY aberration sensor [1] is used to characterize the four AT/UT VLT beams quality and it can also improve the performance of star beam injection into the fiber-fed beam combiner. The aberration sensor is equipped with four Shack-Hartmann lenslets operating in the near-infrared. Each telescope beam wavefront aberrations are measured simultaneously by imaging the Galactic Center field using a Shack-Hartmann. The wavefront aberrations are in general measured in three steps: a) compute the centroids of the Shack-Hartmann spots; b) measure the wavefront slopes by comparing the measured centroids with a reference grid; c) retrieve the aberration coefficients with the computed slopes. The standard point source Shack-Hartmann spot centroids are computed out using a weighted centroid algorithm. Since the aberration sensor Shack-Hartmann images are filled with the crowded Galactic Center objects, the shifts of the distorted images have to be estimated with a correlation algorithm.

We report a simulation of the Shack-Hartmann lenslet images of the Galactic Center. A NACO Galactic Center image was obtained and later it is interpolated to the pixel scale of the aberration sensor. The image was next convolved with the point spread function of the lenslet sub-aperture. The resulted image was then projected on the Shack-Hartmann grid. This image is free of the VLT aberrations.

The accuracy of seven existing correlation centroid algorithms [cf. Tab. 1] [1] for the Galactic Center field is studied numerically. The centroid is computed by finding the mismatch between a reference image and a target image. The reference image should be locally tilt free to get a good centroid estimate. The generation of reference image was accomplished by averaging 50 lenslet sub-aperture images of a single frame.

The comparison of the above algorithms is carried out at different signal to noise ratio levels and known input shifts. From the analysis we found out that the zero mean sum of square difference, sum of square difference are the best in performance in comparison to others. The zero mean sum of square difference performs better than sum of square difference with an additional computational cost. In this work the sum of square difference algorithm was chosen to compute the slopes of the aberration sensor.

Next studied the performance of wavefront aberration measurement accuracy. The absolute wavefront aberration error is defined as the absolute difference between the input wavefront aberration and the measured wavefront aberration. The experimentally measured wavefront aberrations

Table 1: Correlation algorithms, I_0, I_L reference and live images, * is complex conjugation, $\bar{I}_0$ is the mean intensity of I_0.

Name	**Correlation coefficient**
Cross correlation, image domain (CCI)	$\sum I_L(x \pm \Delta x, y \pm \Delta y) \times I_0(x, y)$
Cross correlation, Fourier domain (CCF)	$FT^{-1}\{FT[I_L(x \pm \Delta x, y \pm \Delta y)] \times FT^*[I_0(x, y)]\}$
Sum of square difference (SSD)	$\sum \left[I_L(x \pm \Delta x, y \pm \Delta y) - I_0(x, y)\right]^2$
Zero mean sum of square difference (ZSSD)	$\sum \left[\left(I_L(x \pm \Delta x, y \pm \Delta y) - \bar{I_L}\right) - (I_0(x, y) - \bar{I_0})\right]^2$
Sum of absolute difference function (SAD)	$\sum \left\lvert I_L(x \pm \Delta x, y \pm \Delta y) - I_0(x, y)\right\rvert$
Zero mean sum of absolute difference (ZSAD)	$\sum \left\lvert \left[I_L(x \pm \Delta x, y \pm \Delta y - \bar{I_L}\right] - \left[I_0(x, y) - \bar{I_0}\right]\right\rvert$
Sum of absolute difference squared (SADS)	$\left[\sum \lvert I_L(x \pm \Delta x, y \pm \Delta y) - I_0(x, y)\rvert\right]^2$

were added to the Galactic Centre image in three folds: a) applied the aberrations induced phase in the Fourier plane of the Galactic Centre image; b) shifted the Galactic Center image with the computed slopes from the VLT aberrations induced point source Shack-Hartmann; c) generated the artificial Galactic Centre image by the shift and add method using the VLT aberration induced Shack-Hartmann spots. The methods measures the absolute wavefront aberration with an accuracy better than 100 nm for a 2 s integration (2000 photons/sub-aperture) image.

The GRAVITY calibration unit provides the artificial stars to characterize the performance of the acquisition camera. Two stars were implemented by using the two single mode fibers separated by nearly 1 mm. This corresponds to two stars separated by 1.5" in the sky. The stars beam is reflected by a parabolic telescope is then guided to the acquisition camera by using a set of mirrors [2].

The two star field illuminated aberration sensor images are acquired in the presence of phase screens and also with moving the tip-tilt devices. The performance of the correlation algorithms were analyzed for the experimental aberration sensor image data. The analysis was carried out in four steps: a) generation of the reference image from the target aberration sensor image itself; b) select the known input shifts image (target image); c) apply the correlation algorithm between the reference and the target image. d) repeat above steps for different signal to noise ratio images. The sum of square difference algorithm is the best in performance when compared with others. The experimental aberration sensor image with 2000 photons/sub-aperture allows it to measure the wavefront aberrations with an accuracy better than 250 nm. Presently the optimization work is progressing. The calibration of the software is being adapted with the instrument data.

References

[1] Anugu, N. et al., *Near-infrared aberration tracking using a correlation algorithm on the Galactic Center*, SPIE Astronomical telescopes + Instrumentation, Montreal, Canada, 9148-207 (2014)

[2] Blind, N. et al., *GRAVITY: the calibration unit*, SPIE Astronomical telescopes + Instrumentation, Montreal, Canada, 9146-64 (2014)

Building the GRAVITY instrument for the ESO VLTI

António Amorim[1], Paulo J. V. Garcia[2], Paulo Gordo[1], Narsireddy Anugu[2], Jorge Abreu[1]

[1]*SIM-CENTRA and FCUL – Edifício C8, Campo Grande, P1749016 Lisboa, Portugal*
[2]*SIM-CENTRA and FEUP – Rua Dr. Roberto Frias, s/n, 4200-465 Porto, Portugal*

Abstract

GRAVITY is the second generation VLT Interferometer instrument for precision narrow-angle astrometry (10 microarcseconds resolution) and interferometric imaging. The instrumentation techniques used include fiber-fed integrated optics, wavefront sensors, a fringe tracker, beam stabilization and a novel metrology concept. The VLTI is the largest array of 8-metre telescopes that explicitly included interferometry in its design and implementation, providing six baselines for interferometric measurements that are fully exploited by the R 4000 gravity K band science spectrometer. Several innovative sub-systems are used to make the phase measurements meaningful. Using a reference star, the atmosphere turbulence is compensated by 4 IR wave front sensors actuating the MACAO telescope deformable mirrors, extending the usability of AO to the regions of high obscuration like the Galactic center. Telescope oscillations and tunnel aberrations are corrected by, a laser guiding systems, measurements with the IR acquisition camera (H-band) delivered by our group and a train of fast steering mirrors that tune the light injection in the fibers. The acquisition camera combines and analyses the 4 telescope light with field, pupil, pupil tracking and aberration measurement modes. The K band light is injected into fibers that form fast delay units and deliver the photons to the integrated beam combiner. The development of an integrated optics beam combiner for K band light is a new development for the GRAVITY instrument. In astrometric mode both science and phase reference stars are used to drive the fringe tracker detector and the science spectrometer. Phase differences resulting from open path variations along the optical train up to the telescopes are compensated by measuring at the telescope spiders the interference patterns of laser light back-propagated from the beam combiner instrument.

At present time all systems are integrated in the cryostat and the inter-systems operation is being optimized.

Measurement of the VLT pupil motions using a 2×2 lenslet evaluated aberrations

Narsireddy Anugu[1], Antonio Amorim[2], Paulo Garcia[1], Paulo Gordo[2], Frank Eisenhauer[3], Oliver Pfhul[3], Nicolas Blind[3], Jorge Abreu[2]

[1] *Universidade do Porto, Faculdade de Engenharia, Laboratório SIM Unidade FCT no 4006, Rua Dr. Roberto Frias, s/n, 4200-465 Porto, Portugal*
[2] *SIM and FCUL - Edificio C8, Campo Grande, P1749016 Lisboa, Portugal*
[3] *Max Planck Institute for extraterrestrial Physics, PO Box 1312, Giessenbachstr., 85741 Garching, Germany*

Abstract

A long baseline interferometer can convert the optical path difference into the astrometric measurements. The optical path difference is equal to the scalar product between the baseline vector of the interferometer and the direction of the star in the sky. The optical path difference can be measured using a metrology system between the interferometric lab and to the VLT pupil plane. During the observations the movements of delay line carriages can alter the effective pupil plane. A misalignment between the sky plane and the effective telescope pupil plane can introduce astrometric errors. For example a 4 cm lateral pupil position error at 8 m beam contributes 8 μas astrometric error. Hence the accurate astrometry measurements require an active pupil plane monitoring during the science observations.

The GRAVITY telescope pupil positions are tracked by the acquisition camera pupil tracking imaging mode [2]. The monitoring is implemented by mounting four pupil guiding laser beacons (1.2 μm) on each telescope secondary mirror spiders and later image them using a 2×2 lenslet inside the acquisition camera. The acquisition camera optics allows the VLT lateral and longitudinal pupil shifts to be converted into the beam tip-tilt and defocus aberrations when it is falling on the 2×2 lenslet. The lenslet allows it to measure the first four primary aberrations successfully. These measurements can be related to the pupil lateral and longitudinal positions with the equations given in Anugu et al. (2014).

We report a simulation of 2×2 lenslet images. Experimentally measured optical aberrations were applied in the numerical simulations. The local slopes can be measured by comparing the distorted spot centers with the reference fiber coupler spot centers. Using the slopes, retrieved the first four aberrations in two fronts: a) Zernike method; and b) Salas-Peimbert et al. (2005) method.

In the Zernike method, the wavefront $W(x, y)$ is represented as the linear combination of Zernike polynomials as given in Eq. 1. In the Salas-Peimbert method, the wavefront is represented as given in Eq. 2 and measured the coefficients using analytical equations derived from the spot shifts. Comparison studies reveal that the Zernike method of evaluation is better than the other. The Zernike method is chosen to estimate the aberrations from the slopes.

$$W(x, y) = \sum_{i=1}^{i<=4} A_{\mathrm{i}} Z_{\mathrm{i}} \tag{1}$$

$$W(x, y) = A_1 + A_2 x + A_3 y + A_4(x^2 + y^2) \quad (2)$$

Where A_1, A_2, A_3 and A_4 are the piston, tip, tilt and defocus beam aberrations. And Z_i is the Zernike polynomial for the i^{th} index.

We measured the pupil shifts by simulating the artificial pupil tracker data at various input shifts. We measured the lateral pupil positions with a precision better than 3 mm at 8 m beam and the longitudinal pupil positions with a precision better than 20 mm at 80 mm compressed UT beam.

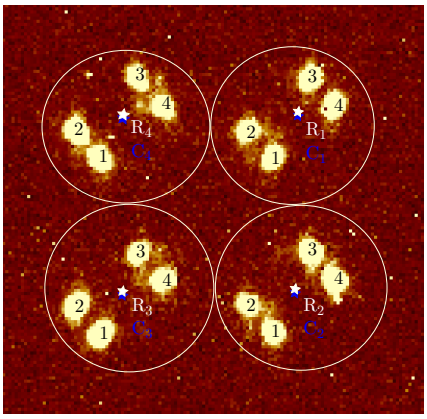

Figure 1: The experimental acquired pupil tracker image.

The GRAVITY calibration unit simulates the artificial telescope and the pupil guiding lasers in the MPE lab. The pupil guiding lasers were implemented by using a multimode fiber laser which illuminates a four hole aluminum mask. The four holes separation corresponds to the actual position of lasers on the VLT secondary mirror spiders. The laser light reflected from the telescope is guided to the four openings of the acquisition camera using the beam splitters and flat mirrors. We acquired the pupil tracker image data with various pupil shifts. The pupil shifts in the instrument are simulated using the pupil motion controllers which are used for the stabilization of the pupil.

As shown in Fig. 1, the spots 1-2-3-4 represents the pupil guiding laser beacons mounted on the telescope. The symbols R_1, R_2, R_3 and R_4 are the reference positions. The C_1 is the barycenter position of 1-2-3-4 laser spots for a single lenslet sub-aperture. The C_2, C_3 and C_4 are the barycenter positions of laser spots for the remaining sub-apertures. In case of lateral pupil shift, the whole barycenters C_i shifts with respect to the reference centers R_i in X or Y directions. A longitudinal shift causes the C_i to diverge/converge with respect to the R_i. In this example one can see the lateral shift along the Y-direction, as the C_i are tilted in Y-direction with respect to the R_i. Using the experimental data, the pupil positions are measured. The pupil position measurement accuracy is within the GRAVITY specifications.

References

[1] Salas-Peimbert, D. et al., *Wave-front retrieval from Hartmann test data*, Applied Optics, Vol. 44, Issue 20, pp. 4228-4238 (2005)

[2] Anugu, N. et al., *The GRAVITY/VLTI acquisition camera software*, SPIE Astronomical telescopes + Instrumentation, Montreal, Canada, 9146-83 (2014)

Design, development and calibration of the GRAVITY acquisition camera software to monitor four telescope beams

Narsireddy Anugu[1], Paulo Garcia[1], Antonio Amorim[2], Paulo Gordo[2], Frank Eisenhauer[3], Oliver Pfhul[3], Nicolas Blind[3], Jorge Abreu[2]

[1] *Universidade do Porto, Faculdade de Engenharia, Laboratório SIM Unidade FCT no 4006, Rua Dr. Roberto Frias, s/n, 4200-465 Porto, Portugal*
[2] *SIM and FCUL - Edificio C8, Campo Grande, P1749016 Lisboa, Portugal*
[3] *Max Planck Institute for extraterrestrial Physics, PO Box 1312, Giessenbachstr., 85741 Garching, Germany*

Abstract

The GRAVITY acquisition camera is a four VLTI beams monitoring instrument, operating in the near-infrared. It has four imaging modes a) field imager: images the H-band science field and tracks the tip-tilt b) pupil tracker: images the pupil guiding laser beacons (1.2 μm) mounted on the secondary telescope using a 2×2 lenslet and tracks the telescope pupil motions c) aberration sensor: images the H-band science field using a 9×9 lenslet and evaluates the beam higher order aberrations d) pupil imager: re-images the telescope pupil with H-band science light. The science field tip-tilts are induced by the tunnel atmosphere. Their measurement is very critical to inject star light into the fiber-fed beam combiner with high coupling efficiency. The pupil tracker measures the lateral and longitudinal pupil motions. These measurements are used to guide the telescope beam in a closed loop. It minimizes the astrometric error by stabilizing the pupil plane with the sky plane. The higher order aberrations are used to characterize the beam quality of the telescope and also used for wavefront correction. The pupil and field images are used to verify the optical alignments and to monitor the pupil and field tracking strategy.

In this communication, a simulation of the acquisition camera system was carried out in the presence of VLTI aberrations. The VLTI aberrations consist of the adaptive optics residuals, slow tunnel seeing induced aberrations and also the optical vibrations, delay line carriages induced optical aberrations. The field imager has been simulated using a NACO Galactic Center image. The experimentally measured VLTI aberrations were introduced to the field imager and measured back with a precision better than 2 mas [**?**]. The atmospheric differential refraction effects were addressed.

The pupil tracker images were simulated by applying the experimentally measured optical aberrations resulting from the movement of delay line carriages. The true lateral pupil positions are measured with a precision of better than 3 mm for an 8 m beam (UT) and the longitudinal pupil position measured with a precision better than 20 mm at 80 mm compressed UT beam respectively. The pupil image is simulated by considering the telescope obstruction along with acquisition camera pupil lens diffraction effects. The aberration sensor consists of a Shack-Hartmann Lenslet array. A point source and Galactic Center aberration sensor artificial images were simulated. The experimentally measured VLT aberrations were applied to the artificial images and reconstructed back the VLT aberrations with an accuracy better than 100 nm for a 2s integration. In Fig. **??** the acquisition camera image for a single telescope is presented.

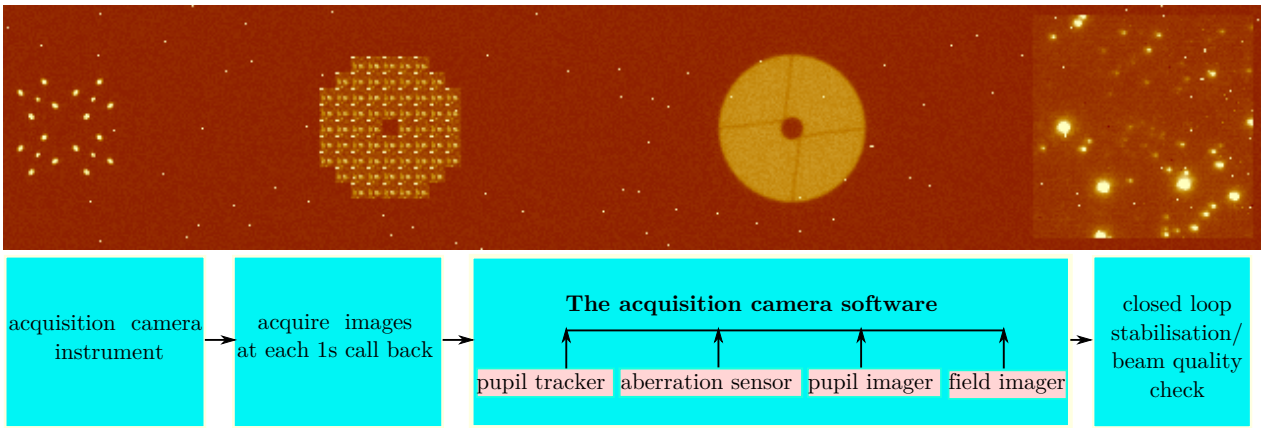

Figure 1: (Upper image) The acquisition camera detector image for a single telescope. The lower flowchart represents the acquisition camera software working flow.

The acquisition camera software is implemented using the ESO software standers and integrated within the GRAVITY software. During the observations, the software triggers automatic callbacks to new image events with a 1 Hz rate. For each call back, the Next Generation Detector acquires a new acquisition camera image and shares the image location with the acquisition camera software. As shown in Fig. **??**, the top level function of the software calls its four low level functions namely the field imager, the pupil tracker, the aberration sensor and the pupil imager. These functions take the respective image windows and extract the aberration parameters simultaneously for all the telescope beams. The estimated aberration parameters are then stored in the instrument database. Those parameters are used to apply the corrections for the pupil position shifts in a closed loop. They also make the light coupling scheme efficient because the parameters are used to apply the tip-tilts to the fiber positions in a closed loop. Furthermore to characterize the telescope beam quality. These software routines work simultaneously on the instrument work station in parallel with science observations. The software has special calibration functions, which is used to calibrate the reference positions automatically.

In the MPE lab, an experimental setup simulates the telescope with the artificial stars and the pupil guiding lasers [**?**]. The experimental image data has been acquired with simulating the pupil shifts, atmospheric effects. Also data has been acquired by varying the star and laser magnitudes. The experimental image data was analyzed. The extracted parameters are within the GRAVITY specifications. Currently the field imager, pupil tracker software are working in a closed loop with the instrument. The aberration sensor is now being adapted to the real instrument data.

References

[1] Anugu, N. et al., *The GRAVITY/VLTI acquisition camera software*, SPIE Astronomical telescopes + Instrumentation, Montreal, Canada, 9146-83 (2014)

[2] Blind, N. et al., *GRAVITY: the calibration unit*, SPIE Astronomical telescopes + Instrumentation, Montreal, Canada, 9146-64 (2014)

Effects of anisoplanatism on the visibility amplitudes and phase variances measured by the PRIMA fringe trackers

Nuno Gomes[1,2], Françoise Delplancke[3]

[1]*Laboratório de Sistemas, Instrumentação e Modelação em Ciências e Tecnologias do Ambiente e do Espaço (SIM)/Faculdade de Engenharia da Universidade do Porto (FEUP), Rua Dr. Roberto Frias, s/n, 4200-465 Porto, Portugal*
[2]*Faculdade de Ciências da Universidade do Porto (FCUP), Rua do Campo Alegre, s/n, 4169-007 Porto, Portugal*
[3]*European Organisation for Astronomical Research in the Southern Hemisphere (ESO), Karl-Schwarzshild-Straße 2, Garching bei München, Germany*

Abstract

During dual-field observations with the VLTI PRIMA facility, the quality of the fringe tracking performed by the fringe sensor unit (FSU) observing the secondary object depends on the angular separation between the two objects being simultaneously observed, the detector integration time (DIT) and the atmospheric observational conditions. The effects of the angular anisoplanatism on the performance of the FSUs in dual-feed are analysed by means of the impact of the angular separation between pairs of unresolved stars on the visibility amplitudes and phase variances measured by the FSUs. The relations between the visibility amplitude, the detector integration time and the light tunnel conditions (temperature and seeing) are studied as well.

Visibilities amplitudes of 1.3 ± 0.3 and 1.2 ± 0.3 where measured respectively for HD18829 and HD15520.[1] These values are compatible with non-resolved stars. The results indicate that although the FSUs were designed to measure the visibility phase only, visibility amplitudes can be reasonably estimated in the astrometric mode. The effects of the anisoplanatism on these measurements can be studied and extrapolated for the case when the FSUs are used as off-axis fringe trackers.

References

[1] Gomes, Nuno; ; Schmid, Christian; Sahlmann, Johannes; Ménardi, Sérge; Abuter, Roberto; Mérand, Antoine; Delplancke, Françoise, "*Estimating visibility amplitudes with the PRIMA fringe trackers*", Optical and Infrared Interferometry III. Proceedings of the SPIE, Volume 8445, article id. 844522, 9 pp (2012).

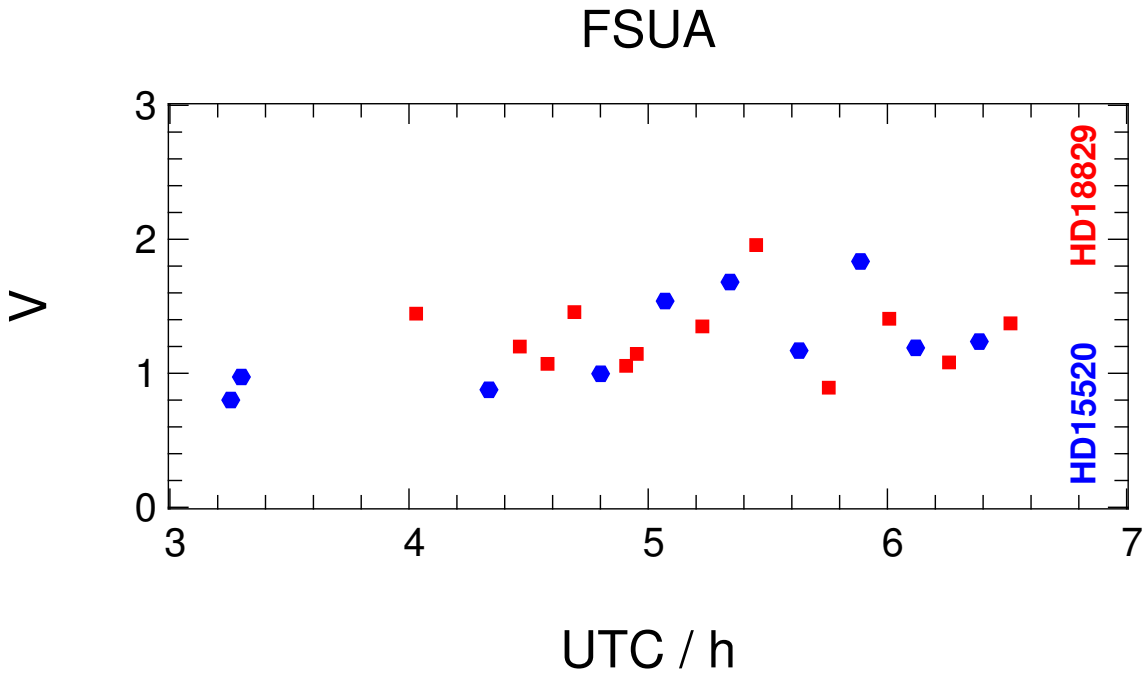

Figure 1: Measured visibility points for HD18829 (red squares) and HD15520 (blue dots). The error bars fit inside the symbols representing the visibility points. The visibilities for HD18829 and HD15520 are respectively equal to 1.3 ± 0.3 and 1.2 ± 0.3. Even being higher than 1, these values are compatible with the visibility expected for non-resolved objects.

A Compact Solar Hard X-ray Polarimeter

Rui M. Curado da Silva[1], J. M. Maia[1,2], E. Caroli[3], Wei Fei[4], O. Limousin[5], J. Marques[1,6], M. Pinto[1], N. Auricchio[3], J. B. Stephen[3], Adriana Garcia[7], Paulo Ribeiro[7], João Fernandes[7], Ricardo Patrício[8]

[1] *Laboratório de Instrumentação e Física Experimental de Partículas, Departamento de Física da Universidade de Coimbra, Portugal*
[2] *Universidade da Beira Interior, Covilhã, Portugal*
[3] *IASF – Sezione di Bologna, CNR, Bologna, Italy*
[4] *National Space Science Center, CAS, Beijing, China*
[5] *CEA/DSM/Irfu/Service d'Astrophysique, F91191, Gif-sur-Yvette, France*
[6] *Centro de Astrofísica da Universidade do Porto, Portugal*
[7] *Observatório Geofísico e Astronómico da Universidade de Coimbra, Portugal*
[8] *Active Space Technologies, 3024-307 Coimbra, Portugal*

Abstract

The universe has been studied in the hard X-ray domain almost exclusively through spectral and timing variability analysis as well as through imaging techniques. By measuring the polarization angle and the polarization degree of source emissions, the number of observational parameters is increased by two allowing better discrimination between different models. Polarimetric observations can provide important information about the geometry, magnetic fields, composition and emission mechanisms in a wide variety of gamma-ray sources such as: pulsars, solar flares, active galactic nuclei, galactic black holes and gamma-ray bursts.[7]

In the hard X-ray domain, no dedicated polarimeters have yet been launched into space. However recent polarimetric measurements were performed using the SPI (Spectrometer on INTEGRAL) and IBIS (Imager on-Board INTEGRAL Satellite) instruments on the Crab and on other few stable and transient (GRBs) sources[3, 5].

Herein we propose a compact CdTe based hard X-ray polarimeter with spectro-imaging capabilities optimized for solar physics, merging the solar physics expertise of Chinese partners with the high energy instrumentation experience of European partners for a common goal. Our purpose is to deploy the first dedicated space polarimeter for hard X-rays, as well as to perform the first polarimetric measurements of Sun solar flare emissions. Measuring the continuum emission polarization will allow establishing important constraints on the emission models. For example, the beaming level of charged particles which produce the Bremsstrahlung radiation could be inferred by polarization. Furthermore, pion decay models are not likely to be compatible with a high degree of polarization measured.[7] Therefore, solar polarization measurements in the 100 keV to 600 keV energy range will be an exceptional breakthrough for solar physics, opening a new window to interpret solar flare dynamics.

European partners have been developing high energy telescope focal plane prototypes with polarimetric capabilities in particular in the framework of two proposals submitted to ESA Cosmic Vision M mission calls (Gamma-Ray Imager in 2007 and DUAL in 2010) [6, 1] and at one proposal at bilateral level with Simbol-X joint CNE and ASI joint mission in 2009.[4] From this heritage, we scaled polarimeter tested and verified concepts into the constraints of this CAS-ESA call.

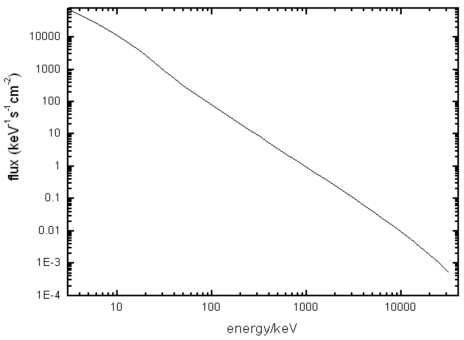

Figure 1: Solar flare hard x-rays emitted by charged particles acceleration.

Since the Sun is the strongest emitter of polarized hard X-rays (fig. 1), a small area ($\sim$12 cm^2), $\sim$2 mm thick, CdTe pixelized matrix ($\sim$3000 sub-millimeter pixels; 500μm size) equipped with a few hundred micron thick tantalum coded mask (allowing imaging up to $\sim$30 keV) should provide high solar photon count rate, for a total mass of about 10 kg and a power electric consumption within 10W. This configuration is intentionally conceived to allow a multi-instrument and multipurpose joint ESA-CAS mission. Such simple configuration together with coincidence electronics allow Compton polarimetry analysis since after undergoing Compton scattering in a matrix pixel, the polarized solar photon's new direction depends on the orientation of its polarization before the interaction. By analysing the Compton photons distribution pattern obtained by a second interaction in the different pixel of the CdTe matrix, a modulation pattern is observed for a polarized solar flux. By both Monte Carlo simulation and prototype experimental testing we showed that a modulation Q factor of about 0.5 is obtained with similar CdTe polarimeter configuration.[2] For a typical solar flare emission whose lifetime may vary from 20 min up to 3 hours, a minimum detectable polarization of about 8% and 3% is estimated for 10 3 s and 10 4 s observation times, respectively, which will allow observing the expected 10 to 25% degree of linear polarization of the whole solar flare loop.

References

[1] P. von Ballmoos, et al., "A DUAL mission for nuclear astrophysics", Experimental Astronomy vol 33, 2012, DOI: 10.1007/s10686-011-9286-6.

[2] R. M. Curado da Silva, E. Caroli, et al., "CIPHER, polarimeter telescope concept for Hard X-ray Astronomy", Experimental Astronomy, Vol. 15, no1, pag. 45-65, (2003).

[3] A. J. Dean, et al, "Polarized gamma ray emission from the CRAB", Science, vol. 321, no 5893, p. 1183 (2008).

[4] Philippe Ferrando et al., "SIMBOL-X: a new-generation hard x-ray telescope", Proc. SPIE 5168, Optics for EUV, X-Ray, and Gamma-Ray Astronomy, 65 (January 29, 2004).

[5] M. Forot, et al., "Polarization of the Crab Pulsar and Nebula as Observed by the INTEGRAL/IBIS Telescope", Ap.J., 688, L29 (2008).

[6] J. Knödlseder, et al, "GRI: focusing on the evolving violent universe", Proc. SPIE on Optics for EUV, X-Ray, and Gamma-Ray Astronomy III, Eds, 6688, p. 668806 (2007).

[7] F. Lei et al., "Compton Polarimetry in Gamma-Ray Astronomy", Space Sci. R., 82, p. 309 (1997).

Wiggly Cosmic String Evolution

J.P.P. Vieira[1,2], C.J.A.P. Martins[2], E.P.S. Shellard[3]

[1] *Faculdade de Ciencias, Universidade do Porto, Rua do Campo Alegre, 4150-007 Porto, Portugal*
[2] *Centro de Astrofísica, Universidade do Porto, Rua das Estrelas, 4150-762 Porto, Portugal*
[3] *Department of Applied Mathematics and Theoretical Physics, Centre for Mathematical Sciences, University of Cambridge, Wilberforce Road, Cambridge CB3 0WA, United Kingdom*

Abstract

The Velocity-dependent One-Scale model (VOS) is a simplified but quantitative analytic model for cosmic string evolution, which accurately captures the behaviour of the network across early regimes with frictional damping and the important matter-radiation transition. Nevertheless, despite its remarkable performance when it comes to calculating large-scale qualitative properties of a string network, it is intrinsically limited in how much it can tell us about the small-scale structure. In this talk, a natural generalisation of the VOS which takes into account the evolution of small-scale structure will be introduced. The main challenges to the development of this novel approach will be discussed, as well as the insight provided by its application to a number of physically relevant limits.

This work is available online at arXiv:1405.7722

This work was done in the context of project PTDC/FIS/111725/2009 (FCT, Portugal). CJM is also supported by an FCT Research Professorship, contract reference IF/00064/2 012, funded by FCT/MCTES (Portugal) and POPH/FSE (EC). JPV is supported by the Gulbenkian Fundation through Programa de Estímulo à Investigação 2013, grant number 132590.

Effects of Biases in Domain Wall Network Evolution

Inês S. C. R. Leite[1,2], Carlos J. A. P. Martins[1], José R. C. C. C. Correia[1,2]

[1] *Centro de Astrofísica, Universidade do Porto, Rua das Estrelas, 4150-762 Porto, Portugal*
[2] *Faculdade de Ciências, Universidade do Porto, Rua do Campo Alegre 687, 4169-007 Porto, Portugal*

Abstract

We study the evolution of various types of biased domain wall networks in the early universe. We carry out larger numerical simulations than those currently available in the literature and provide a more detailed study of the decay of these networks, in particular by explicitly measuring velocities in the simulations. We also use the larger dynamic range of our simulations to test previously suggested decay laws for these networks, including an ad hoc phenomenological fit to earlier simulations and a decay law obtained by Hindmarsh through analytic arguments. We find the latter to be in good agreement with simulations in the case of a biased potential, but not in the case of biased initial conditions.

All of our research can be found in a paper published at Phys Rev D90 (2014) 023521 also available at arXiv:1407.3905.

This work was done in the context of the project PTDC/FIS/111725/2009 from FCT (Portugal). C.J.M. is also supported by an FCT Research Professorship, contract reference IF/00064/2012, funded by FCT/MCTES (Portugal) and POPH/FSE (EC).

Consistency tests of the stability of fundamental couplings and unification scenarios

M.C. Ferreira 1[1,2], O. Frigola[2,3], C.J.A.P. Martins[1], A.M.R.V.L. Monteiro[1,2], J. Solà[4]

[1] *Centro de Astrofísica, Universidade do Porto, Rua das Estrelas, 4150-762 Porto, Portugal*
[2] *Faculdade de Ciências, Universidade do Porto, Rua do Campo Alegre, 4150-007 Porto, Portugal*
[3] *Institut S'Agulla, Carretera de Malgrat 13, 17300 Blanes, Spain*
[4] *Institut Manuel Blancafort, Avinguda 11 de Setembre 29, 08530 La Garriga, Spain*

Abstract

The stability of nature's fundamental couplings is among the most profound open issues in astrophysics and fundamental physics, and has been identified by ESA and ESO as one of the key drivers for the next generation of ground and space-based facilities. At a phenomenological level, fundamental couplings *run* with energy and in many extensions of the standard model, particularly in theories with additional space-time dimensions, they also *roll* in time and *ramble* in space.

A detection of varying fundamental couplings will be revolutionary: it will prove that the Einstein Equivalence Principle is violated. However, improved null results are also important because they will tighten constraints on fundamental physics and cosmology.

Any Grand-Unified model predicts a relation between the variation of α and those of μ and other couplings, and therefore simultaneous measurements of both provide key consistency tests.

We shall work on the assumption that varying fundamental couplings are due to a dynamical, dilaton-type scalar field. We consider a class of grand unification models where the weak scale is determined by dimensional transmutation and the relative variation of all the Yukawa couplings is the same.

With these assumptions one finds that $\frac{\Delta\mu}{\mu} = [0.8R - 0.3(1+S)]\frac{\Delta\alpha}{\alpha}$ where R and S are phenomenological (model-dependent) parameters.

Different combinations of α, μ and g_p can be measured in the radio band. A joint analysis of this dataset can be done to find the most likely values of each one. Figure 1 shows the one-dimensional likelihood contours for each of these parameters. At 68.3% confidence level we find $\frac{\Delta\alpha}{\alpha} = -2.7 \pm 2.2$ ppm, $\frac{\Delta\mu}{\mu} = -1.1 \pm 1.8$ ppm and $\frac{\Delta g_p}{g_p} = 3.5 \pm 5.8$ ppm. In doing this we are neglecting a possible redshift dependence of the variations; more data would allow a more detailed analysis.

By using the phenomenological parametrizations introduced in fifth paragraph, it is possible to translate the available measurements into constraints on the $R - S$ plane which clearly show a degeneracy direction,*i.e.*, these measurements constrain a particular combination of the parameters R and S. At 68.3% confidence level we find $R = 237 \pm 86$ and $S = 630 \pm 230$.

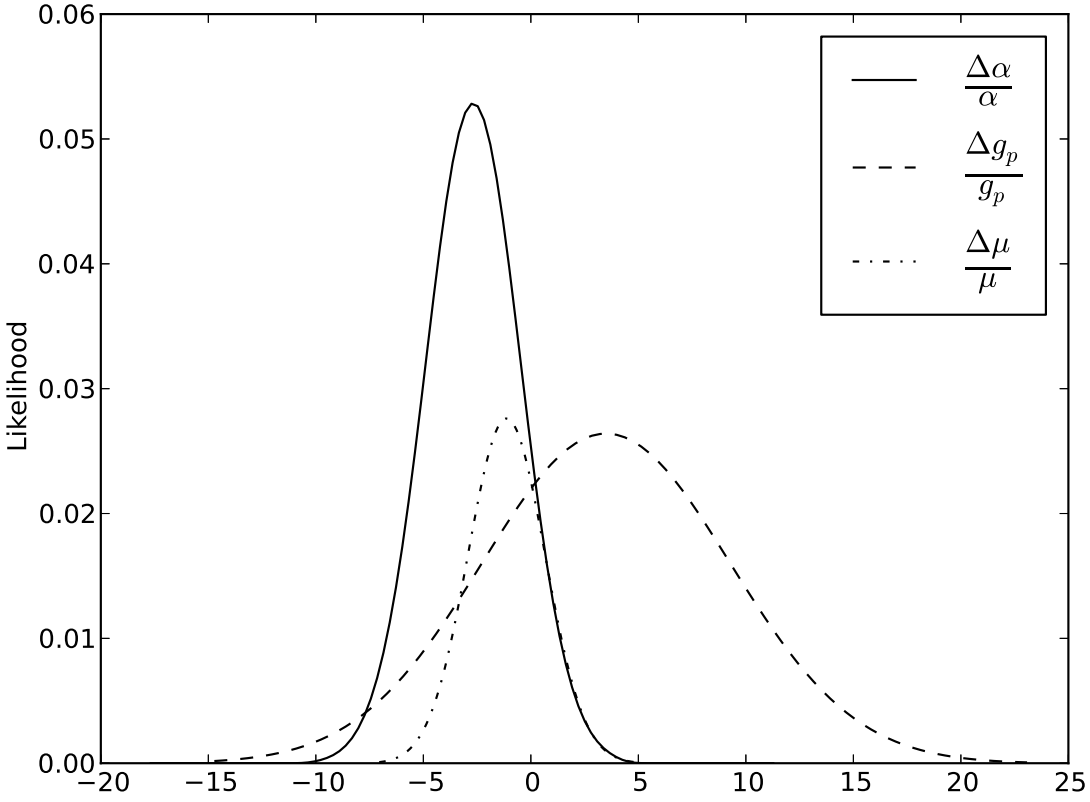

Figure 1: One-dimensional likelihoods for the relative variations of α, μ and g_p from the radio band dataset.

Fundamental Cosmology from Precision Spectroscopy: Varying Couplings

Ana C. O. Leite[1,2], Carlos J. A. P. Martins[2], P. O. J. Pedrosa[1,2]

[1] *Faculdade de Cências, Universidade do Porto, Rua do Campo Alegre, 4150-007 Porto, Portugal*
[2] *Centro de Astrofísica, Universidade do Porto, Rua das Estrelas, 4150-762 Porto, Portugal*

Abstract

The observational evidence for the acceleration of the universe demonstrates that canonical theories of cosmology and particle physics are incomplete, if not incorrect, and that new physics is out there, waiting to be discovered.

Forthcoming high-resolution ultra-stable spectrographs will play a crucial role in this quest for new physics, by enabling a new generation of precision consistency tests. Here we focus on astrophysical tests of the stability of nature's fundamental couplings, and by using Principal Component Analysis techniques further calibrated by existing VLT data we discuss how the improvements that can be expected with ESPRESSO and ELT-HIRES will impact on fundamental cosmology.

We are grateful to Stefano Cristiani, Paolo Molaro, Michael Murphy and John Webb for many interesting discussions and suggestions. Special thanks to Michael Murphy for providing us with the observation times for the VLT sources. We acknowledge the financial support of grant PTDC/FIS/111725/2009 from FCT (Portugal). C.J.M. is also supported by an FCT Research Professorship, contract reference IF/00064/2012, funded by FCT/MCTES (Portugal) and POPH/FSE (EC).

Large-scale magnetic field generation via electron-scale instabilities in unmagnetised shear flows

E. P. Alves[1], T. Grismayer[1], R. A. Fonseca[1,2], L. O. Silva [1]

[1] *GoLP/Instituto de Plasmas e Fusão Nuclear, Instituto Superior Técnico, Lisboa, Portugal*
[2] *DCTI/ISCTE, Lisboa, Portugal*

Abstract

Strong velocity-shear regions found in astrophysical jets constitute important dissipation sites, where plasma kinetic energy is transformed into electric and magnetic field energy via the operation of shear instabilities; these self-generated fields are crucial ingredients for the production of non thermal radiation and accelerated particles. Shear-driven plasma instabilities have generally been studied within the magnetohydrodynamic (MHD) framework, having overlooked the physics at the electron-scale. In this work, we show that a rich variety of electron-scale processes can be triggered in the presence of velocity shear, including the electron-scale Kelvin-Helmholtz instability (ESKHI), the mushroom instability (MI) and a dc-magnetic field generation mechanism. While the ESKHI has a macroscopic analogue in MHD, the latter two processes are not captured in MHD, since these rely on the separate dynamics between electrons and ions.

We have developed the linear theory for the ESKHI and MI, allowing to analytically calculate the linear growth rates and fastest growing modes of these instabilities. The ESKHI modes occur along the flow direction whereas the MI modes develop perpendicular to the flow. We have analysed the effect of a density jump between the shearing flows and found that the operation of these instabilities are robust to extreme density contrasts ($n_1/n_2 \sim 100$). This indicates that these instabilities can be triggered in a wide range of scenarios: in internal shears of the ejecta, where similar density flows interact, and even external shears between the ejecta and the ambiente medium, where large density contrasts come into play. In addition, we have found that the ESKHI and MI growth rates have very different dependencies on the shear flow Lorentz factor (γ_0). The ESKHI growth rate scales as $\gamma_0^{-3/2}$ while the MI scales as $\gamma_0^{-1/2}$. The rapid decay of the ESKHI at high Lorentz factors makes the MI the dominant instability for very relativistic shears.

We have performed multidimensional particle-in-cell (PIC) simulations using OSIRIS in order to verify our theoretical framework. Theoretical predictions are found to be in agreement with numerical simulations. Full 3D simulations also reveal the interplay between the competing ESKHI and MI, confirming the dominance of the MI (ESKHI) for relativistic (sub relativistic) shear flow configurations. Furthermore, numerical PIC simulations allow to probe the nonlinear evolution of these instabilities, which show the generation of electron mixing and turbulence at the shear interface. The electron mixing between shearing flows results in a strong dc-current imbalance on either side of the shear interface (due to the large inertia of the background streaming ions), which, in turn, induces a large-scale dc-magnetic field along the shear interface. This dc-magnetic field structure persists for very long spatial and temporal scales, much larger than the electronic scales, and reaches near-equipartition levels (i.e. ratio of generated magnetic field energy to initial particle kinetic energy on the order of $10^{-3} - 10^{-2}$).

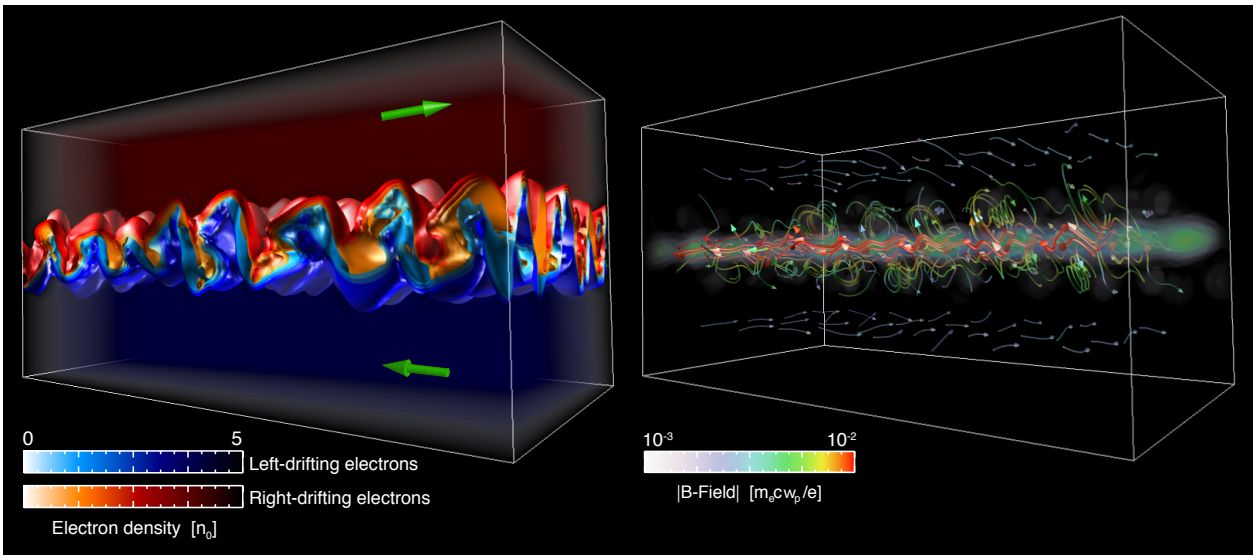

Figure 1: Electron density structures (left) and generated magnetic field (right) due to the self-consistent development of electron shear instabilities (ESKHI in the longitudinal direction and MI in the transverse direction to the flow). The initial flow velocities are $\pm 0.2\ c$.

The development of these shear instability-generated fields will lead to distinct radiation emission signatures and nonthermal particle distributions, which we will further investigate in future work.

References

[1] E. P. Alves, T. Grismayer, S. F. Martins, F. Fiza, R. A. Fonseca, L. O. Silva, Astrophysical Journal Letters, 746, L14 (2012)

[2] T. Grismayer, E. P. Alves, S. F. Martins, F. Fiza, R. A. Fonseca, L. O. Silva, Physical Review Letters, 111, 015005 (2013)

[3] T. Grismayer, E. P. Alves, R. A. Fonseca, L. O. Silva, Plasma Physics and Controlled Fusion, 55, 124031 (2013)

[4] E. P. Alves, T. Grismayer, R. A. Fonseca, L. O. Silva, New Journal of Physics, 16, 035007 (2014)

Fine-structure constant constraints on Bekenstein-type models

P. M. M. Leal[1,2], C. J. A. P. Martins[1], L. B. Ventura[1,2]

[1] *Centro de Astrofísica, Universidade do Porto, Rua das Estrelas, 4150-762 Porto, Portugal*
[2] *Faculdade de Ciências, Universidade do Porto, Rua do Campo Alegre, 4150-007 Porto, Portugal*

Abstract

Astrophysical tests of the stability of dimensionless fundamental couplings, such as the fine-structure constant α, are an area of much increased recent activity, following some indications of possible spacetime variations at the few parts per million level. Here we obtain updated constraints on the Bekenstein-Sandvik-Barrow-Magueijo model, which is arguably the simplest model allowing for α variations. Recent accurate spectroscopic measurements allow us to improve previous constraints by about an order of magnitude. We briefly comment on the dependence of the results on the data sample, as well as on the improvements expected from future facilities.

Acknowledgements

This work was done in the context of project PTDC/FIS/111725/2009 (FCT, Portugal). CJM is also supported by an FCT Research Professorship, contract reference IF/00064/2012, funded by FCT/MCTES (Portugal) and POPH/FSE (EC).

References

http://arxiv.org/abs/1407.4099;
http://dx.doi.org/10.1103/PhysRevD.90.027305

Evolution of the fine-structure constant in quintessence-type models

R.F.C. Alves[1,2], C.J.A.P. Martins[2], A.M.M. Pinho[1,2]

[1] *Faculdade de Ciências da Universidade do Porto, Rua do Campo Alegre, 4150-007 Porto, Portugal*
[2] *Centro de Astrofísica da Universidade de Porto, Rua das Estrelas, 4150-762 Porto, Portugal*

Abstract

We study the cosmological dynamics of representative classes of dynamical dark energy models where the dynamical degree of freedom responsible for the dark energy is coupled to the electromagnetic sector of the theory, and thus leads of variations of the fine-structure constant. We compare the dynamics of the fine-structure constant in these various models, and in particular discuss the role of the onset of the dark energy domination phase (which occurs at low redshift) in this dynamics.

This work was done in the context of project PTDC/FIS/111725/2009 (from FCT, Portugal). CJM is also supported by an FCT Research Professorship, contract reference IF/00064/2012, funded by FCT/MCTES (Portugal) and POPH/FSE (EC).

Fine-structure constant constraints on quintessence-type models

Ana Marta Pinho[1], Carlos Martins[1], Rui Alves[1]

[1] *Centro de Astrofísica da Universidade do Porto, Portugal*

Abstract

Recent spectroscopic measurements suggest a possible parts-per-million cosmological variation of the fine-structure constant. We use these measurements, alone and in combination with Hubble parameter data, to constrain typical classes of dynamical dark energy models where the underlying scalar field also couples to the electromagnetic sector. In particular we highlight how the constraints on the coupling parameter depend on the choice of fiducial cosmological model.

Disformal transformation of cosmological perturbations

Masato Minamitsuji [1]

[1] *Multidisciplinary Center for Astrophysics (CENTRA), Instituto Superior Técnico, Lisbon 1049-001, Portugal.*

Abstract

The Concordance Model of Cosmology has succeeded in explaining the history of the universe, but we still do not understand which fundamental physics is behind it. Gravitational physicists have explored the possible modifications of general relativity on cosmological scales, as the alternatives to the Concordance Model. A naive modification of general relativity provides ghost degrees of freedom arising from the higher derivative terms as well as inconsistencies with experimental tests on general relativity. To avoid the appearance of the ghost degrees of freedom, the equations of motion should be given by the second order differential equations. On the other hand, to pass the experimental tests on general relativity, a realistic modification of gravity should contain a mechanism to suppress scalar interactions on small scales. Recently, it has turned out that successful models of the modified gravity can be described by a class of Honrdeski's scalar-tensor theory, which was originally proposed by Hordenski forty years ago and has been reformulated with the growing interests in applications to cosmological problems. Horndeski's theory is known as the most general scalar-tensor theory where the equations of motion remain of the second order, despite the existence of the higher derivative interactions.

So far, most of studies on Horndeski's theory have focused on the case that the scalar field is minimally coupled to matter. In a generic scalar-tensor theory of gravitation, however, we may consider the situation that the scalar field is directly coupled to the matter sector. In such a case, matter does not follow geodesics associated with the gravitational metric $g_{\mu\nu}$ but that associated with the other metric $\bar{g}_{\mu\nu}$ which differs from $g_{\mu\nu}$ by the contributions of the scalar field. The most familiar case is that the mettric for matter is conformally related to the gravity frame one by $\bar{g}_{\mu\nu} = \alpha(\phi) g_{\mu\nu}$. The gravity and matter frames, $g_{\mu\nu}$ and $\bar{g}_{\mu\nu}$, are often referred to as the Einstein and Jordan frames, respectively. Conformal transformation does not modify the causal structure of the spacetime.

In case of Hordeski's scalar-tensor theory, however, the conformal relation does not provide the most general relation between two metrics. As more general relation between two metrics, we may consider the matter frame metric which is constructed from the derivatives of the scalar field as well as the gravitational metric, $\bar{g}_{\mu\nu} = \bar{g}_{\mu\nu}(g_{\mu\nu}, \phi, \partial\phi, \partial^2\phi, \cdots)$. A naive introduction of higher derivative couplings would, of course, induce ghost instabilities. Thus it would be reasonable to consider that the matter frame metric $\bar{g}_{\mu\nu}$ contains at most the first order derivatives of the scalar field, which is given by $\bar{g}_{\mu\nu} = \alpha(X, \phi) g_{\mu\nu} + \beta(X, \phi)\phi_\mu\phi_\nu$, where $\phi_\mu = \nabla_\mu\phi$ is the covariant derivative of the scalar field associated the gravity frame metric $g_{\mu\nu}$ and $X := -\frac{1}{2} g^{\mu\nu}\phi_\mu\phi_\nu$. Such a generalized relation is often called the disformal relation. However, the gravitational theory written in terms of the matter frame metric $\bar{g}_{\mu\nu}$ could contain terms absent in Horndeski's theory. But the appearance of ghosts would be avoided by the implicit constraints, implying the existence of the healthy scalar-tensor theory beyond Horndeski's theory. In this work, we will focus on the simpler class of the disformal relation $\bar{g}_{\mu\nu} = \alpha(\phi) g_{\mu\nu} + \beta(\phi)\phi_\mu\phi_\nu$ where the gravitational action written in terms of

the matter frame metric $\bar{g}_{\mu\nu}$ also belongs to a class of Horndeski's theory. In contrast to conformal transformation, disformal transformation may change the causal structure of spacetime.

It is well-known that observables must be conformally invariant, irrespective of the choice of the 'physical' frame. If the scalar field is responsible for density perturbations, curvature perturbation in the comoving or uniform energy density gauge, which is conserved after the scales of interest exit the horizon and directly related to the Cosmic Microwave Background anisotropies, is conformally invariant for all orders of perturbations. This fact allows us to evaluate it in the convenient Einstein frame, even though the physical frame is the Jordan frame. The purpose of this work is to extend the analyses on conformal invariance of cosmological perturbations to the case that two metrics are related by disformal transformation.

First, we investigate whether curvature perturbation in the comoving gauge to the scalar field is invariant under disformal transformation as the extension of the well-known invariance under conformal transformation. If it is disformally invariant, it may be evaluated in any disformally-related frame as usually done in the Einstein frame in the gravitational theory with the nonminimal coupling of the scalar field to the Ricci scalar or in the $f(R)$ theory. Second, we will consider the case that disformally coupled matter also contributes to curvature perturbation. In such a case, curvature perturbation will not be conserved due to the existence of isocurvature modes between the scalar field and matter. As in the simple inflation model driven by the disformally coupled scalar field, in some cases matter may be the dominant source of density perturbations via the curvaton mechanism. Such a model may be naturally extended to the case of Horndeski's theory. In each frame, in order to evaluate the final amplitude of cosmological observables, we need to follow the time equation of curvature perturbation on the uniform matter energy density gauge. We will derive the evolution equations of curvature perturbations in the uniform matter energy density gauges in both the gravity and matter frames in the presence of the disformal coupling. In general, notion of adiabaticity in both frames does not coincide, and in the gravity frame curvature perturbation is not conserved even though matter satisfies the adiabaticity condition. We will also derive the formula relating curvature perturbations in both frames.

Latest results from EULAG-MHD global 3D MHD simulations of solar convection and dynamo action

Dário Passos[1,2,3], Paul Charbonneau[2]

[1] *CENTRA, Instituto Superior Técnico, Universidade de Lisboa, Av. Rovisco Pais, 1049-001 Lisboa, Portugal*
[2] *GRPS, Départment de Physique, Université de Montréal, C.P. 6128, Centre-ville, Montréal, Qc, Canada H3C-3J7*
[3] *Departamento de Física, Universidade do Algarve, Campus de Gambelas, 8005-139 Faro, Portugal*

Abstract

The holy grail of space weather is to be able to accurately predict the behavior of the solar magnetic field. Unfortunately the main theory behind the origin of the solar cycle is primarily explanatory and still far from predictive. Nevertheless new tools are being developed that might change this picture over the coming decade. The steady advance in computer power has finally enabled us to explore the solar dynamo problem by means of 3D global magnetohydrodynamical (MHD) simulations of the convection zone. Using the EULAG-MHD code [Smolarkiewicz & Charbonneau 2013], we have succeeded in producing simulations of the Sun's magnetic activity cycles that resemble the observed evolutionary patterns of the large-scale solar magnetic field; most notably regular magnetic polarity reversal occurring on a decadal timescale [Ghizaru *et al* 2010]. These simulations solve the anelastic form of the ideal MHD equations in a thick, rotating shell of electrically conducting fluid, the outer two thirds of which unstably stratified and subjected to thermal forcing. Since these simulations are fully dynamical in all time and spatial resolved scales, they achieve highly turbulent regimes and naturally produce variable amplitude solutions. We have recently been able to produce a simulation that spans for 1650 years and that produced 40 complete sunspot like cycles, the longest of its kind so far. This allows to perform statistical studies and direct comparisons with the observed solar cycle [Passos & Charbonneau 2014]. Some of the main similarities and differences between the statistical properties of simulated and observed cycles are presented here (e.g. evidence for Gnevyshev-Ohl patterns, Gleissberg modulation or hemispheric coupling). Additionally, by studying the behaviour of the large scale flows in the simulation (differential rotation and meridional circulation) we also find evidence for solar cycle modulation of the deep equatorward flow in the meridional circulation [Passos *et al* 2014]. This result is briefly discussed as well as its implications for current helioseismic measurement methodologies and for classical kinematic mean-field flux transport dynamo simulations.

References

[Ghizaru *et al* 2010] Ghizaru, M., P. Charbonneau, P.K. Smolarkiewicz, 2010: Astrophys. J. Lett., 715, L133

[Passos & Charbonneau 2014] Passos, D., Charbonneau, P., 2014, A&A (in press) 2014

[Passos *et al* 2014] Passos, D., Charbonneau, P., Miesch, M., 2014, ApJL (in preparation) 2014

[Smolarkiewicz & Charbonneau 2013] Smolarkiewicz, P.K., Charbonneau, P., 2013, J. Comput. Phys., 236, 608-623

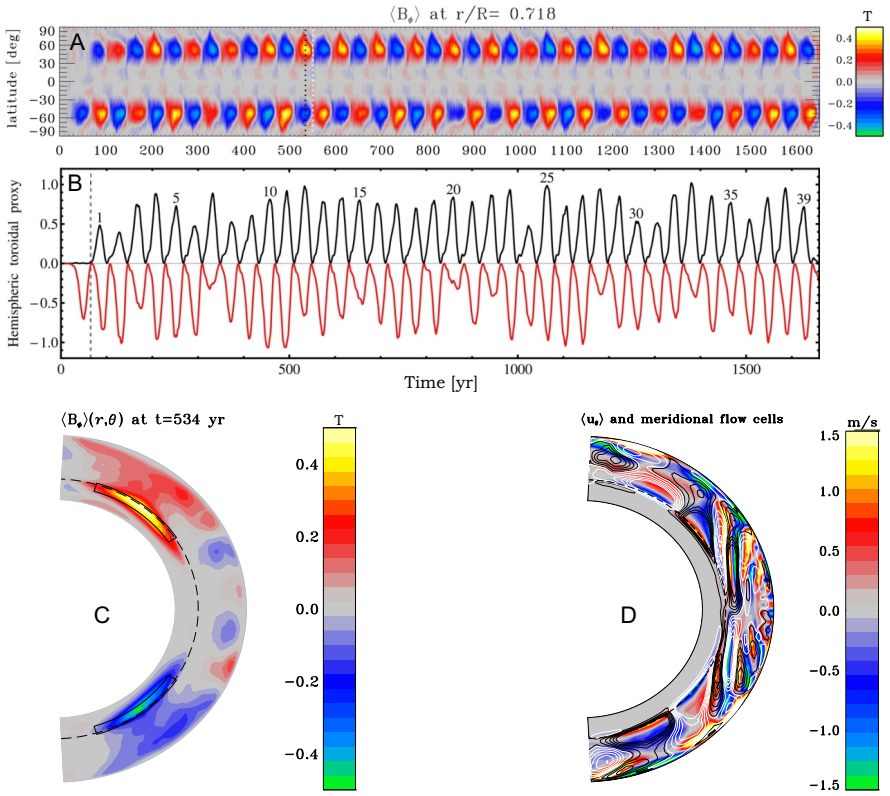

Figure 1: The *millennium simulation* spans for 1650 years and produced 40 large scale field polarity reversals. **A)** Time vs. Latitude diagram of the zonally averaged toroidal field sampled near the tachocline depth. **B)** Time series representing the solar cycle equivalent in the simulation, for the northern (black) and southern (red) hemispheres. The south hemisphere is plotted with a negative sign to facilitate the comparison of the timing of minima. The time series is obtained by integrating the toroidal field, $\langle B_\phi \rangle$ over the area where it accumulates and depicted by black boxes in C). The simulated cycles are numbered for reference. A meridional snapshot of $\langle B_\phi \rangle$ taken at cycle 12 maximum is shown in **C)**. The black dashed line represents the tachocline. In this simulation $\langle B_\phi \rangle$ accumulates at mid latitudes and just below the interface between the unstable convection zone and the stably stratified layers. **D)** meridional plot of the $\langle u_\theta \rangle$ component of the large scale flow. Poleward flows are positive. The cellular topology of the meridional circulation is superimposed on the figure. White (black) lines represent the counter-clockwise (clockwise) rotating cells.

Empirical solar/stellar cycle simulations

Ângela Santos[1,2], Margarida Cunha[1], Pedro Avelino[1,2]

[1]*Instituto de Astrofísica e Ciências do Espaço, Universidade do Porto, CAUP, Rua das Estrelas, PT4150-762 Porto, Portugal*
[2]*Departamento de Física e Astronomia, Faculdade de Ciências, Universidade do Porto, Rua do Campo Alegre 687, PT4169-007 Porto, Portugal*

Abstract

In the Sun, as a result of the solar dynamo, the level of magnetic activity varies according to the 11-year solar cycle. The changes in the overall magnetic field are accompanied by a periodic variation of the number of emerging sunspots, the total area covered by them and the gradual equatorward migration of sunspots. Likewise, the properties of solar oscillations, in particular frequencies and amplitudes, are observed to vary over the solar cycle. However, it is still not clear to what degree these variations result from the direct effect of the sunspots on the propagation properties of the acoustic waves. With the recent discovery of manifestations of activity cycles in the the asteroseismic data of other stars, and the consequent perspective of studying stellar dynamos under different conditions, the understanding of how different agents contribute to the activity-related variations in the properties of stellar oscillations becomes even more important.

The primary objective of the work presented here is to build an empirical model capable of simulating the main characteristics of the distribution of sun/stellar spots over an activity cycle. In order to reproduce the sunspot properties, we base our model on observational constraints deduced from solar data (NOAA/NGDC), such as number of sunspot groups, the sunspot's areas and lifetimes, the formation latitude and the sunspot's angular velocity. We started by a simple toy model and gradually increased its complexity in order to improve the simulations. In what follows I briefly summarize the input parameters of the current version of the model.

The number of emerging sunspots increase as the level of magnetic activity increase. Moreover, the rising phase of the cycle is faster than the declining phase, thus the solar cycle has an asymmetric shape. Our empirical model considers sunspot groups as independent events. At each time step, the number of generated groups, N, is randomly determined by a Poisson distribution with a mean value $N_{\rm m}$, which is based on a function that fits the daily number of observed sunspot groups.

The sunspot formation zone also varies over the cycle. The spots of a cycle start to emerge at latitudes about $\pm 40^{\circ}$. As the cycle proceeds the spots form at progressively lower latitudes. Around the activity minimum, while the last spots of the previous cycle form at $\pm 5^{\circ}$, the first spots of the new cycle emerge at hight latitudes (i.e. consecutive cycles may overlap). Besides, this equatorward drift of the mean latitude of spots, the width of the formation zone also varies. Therefore, our model determines randomly the latitude of each generated group through a Gaussian distribution with parameters $L_{\rm m}$ and $\sigma_{\rm L}$. The mean latitude $L_{\rm m}$ is determined from the fit to the sunspot latitudes with an exponential function, while $\sigma_{\rm L}$ is assumed to be a constant before the maximum and, after that, a decreasing linear function with the activity level.

The area distribution of sunspot groups can be described by a log-normal distribution. Therefore, the area of each group is determined randomly through a log-normal distribution, which fits

the observed area distribution. The group lifetime depends on its size. This relation is described by the Gnevyshev-Waldmeier (GW) rule, where the maximum area of the group/spot is proportional to the lifetime. However, we found that the Gnevyshev-Waldmeier rule is not valid for small groups (< 40MSH; MSH is 10^{-6} of solar hemisphere), which should live longer than predicted by this rule. After several attempts, we verified that by assuming an exponential function for small groups, our model reproduces the observed properties of the solar cycle.

The daily sunspot records correspond only to the visible side of the Sun. Therefore, in our model we take into account the solar rotation. Although the spots rotate slightly faster than the solar surface, we assume that the difference is not significant and, hence, the adopted sunspots' rotation follows the surface rotation. The position in longitude for each group is randomly determined from an uniform distribution. By taking the group's angular velocity and lifetime into account, the model determines when the group is visible.

Figure 1 shows the results of a simulation obtained with the current version of the model, which reproduce reasonably well the properties of the sunspot cycle as can be seen in the figure.

It is our intention, at a later stage, to reduce the model complexity to simulate cycles of other solar-like stars, from which much less information is available.

We also derived a model to infer the frequency shifts induced by spots. The simulations can then be used to estimate the spots' impact on the oscillation frequencies. In this conference, we present a preliminary comparison of the simulated frequency shifts with the frequency shifts observed over the solar cycle.

Finally, we note that this kind of simulations may have other applications, such as in the study of radial velocity signals for exoplanet search. In particular, the simulations may help designing strategies to reduce the signatures induced by stellar activity in the radial velocity.

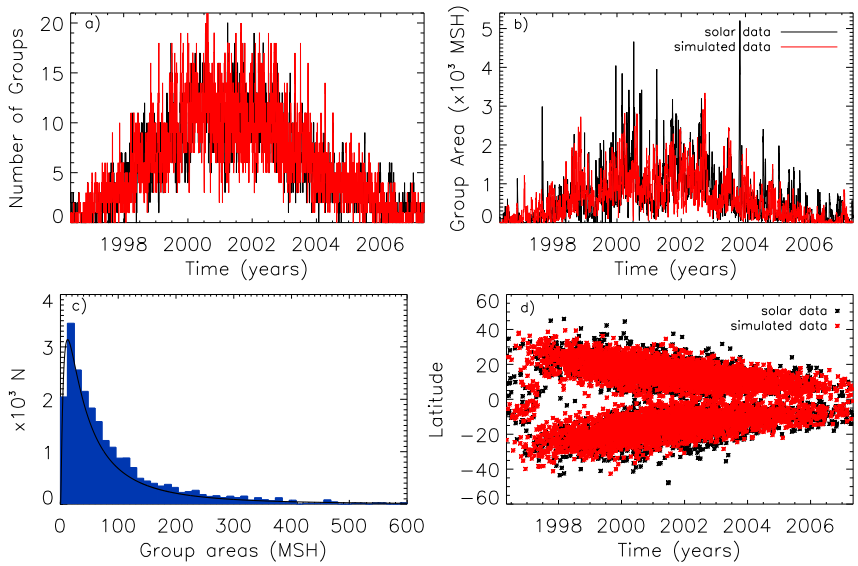

Figure 1: Results of one of the simulations obtained with the empirical model of the solar cycle. The real solar data is shown in black and the simulation in red. a) Number of sunspot groups over the solar cycle 23. b) Total area covered by spots. c) Area distribution of simulated groups (blue) and log-normal fit to the solar data (black). d) Latitudinal distribution of sunspot groups.

The interesting case of HD41248: stellar activity, no planets?

João Faria[1,2] *

[1] *Instituto de Astrofísica e Ciências do Espaço, Universidade do Porto, CAUP, Rua das Estrelas, PT4150-762 Porto, Portugal*
[2] *Departamento de Física e Astronomia, Faculdade de Ciências, Universidade do Porto, Rua do Campo Alegre 687, PT4169-007 Porto, Portugal*

Abstract

Several studies on solar neighbourhood stars have shown that the frequency of giant planets is a strong function of the stellar metallicity. It is easier to find such a planet around a metal-rich star than around a metal-poor object [2, 3, 4]. This observational result is usually interpreted as due to a higher probability of forming a giant-planet core before the dissipation of the proto-planetary disk in a metal-rich environment. A number of questions are still open, however, whose answer may have strong implications for planet formation models, especially in the metal-poor regime.

To our knowledge, no specific radial velocity (RV) survey for Neptunes and super-Earths orbiting low-metallicity stars has been carried out. To address this problem, we started a dedicated programme using the HARPS spectrograph at the 3.6-m ESO telescope (La Silla Paranal Observatory, Chile) for a total of 80 nights over three years (starting in October 2012) within an ESO Large Program (190.C-0027). When this programme is completed, we expect to be able to derive the frequency of Neptunes and super-Earths in the metal-poor regime and compare it with the published results for solar metallicity stars and with the model predictions [5].

In a recent paper, Jenkins et al. (2013) used the first 62 (public) RV measurements of the star HD 41248 to announce the detection of a system of two super-Earth or Neptune-mass planets with orbital periods of 18.36 and 25.65 days. We present a detailed analysis of 162 additional RV measurements of HD 41248, obtained within the Large Program, with the goal of confirming the existence of the proposed planetary system. We analysed the precise radial velocities (with a timespan of over 10 years) together with several stellar activity diagnostics and line profile indicators.

The results of this analysis do not allow the confirmation of the planetary origin of the signals suggested by Jenkins et al. (2013). The observed 25-day-period signal is almost exactly reproduced in the stellar activity index $\log R'_{HK}$ and in the FWHM of the HARPS CCF (see Fig. 1). Although we cannot fully discard the existence of a stable, periodic signal at 18 days, as expected from the presence of a planet, different tests show that the current data (both the RV and activity/line-profile indicators) do not support its existence.

The complexity of the signals and the estimate for the rotational period of the star ($\sim$20 days) lead us to propose that the observed 18-day and 25-day signals may be caused by at least two different active regions in a star presenting a strong differential rotation pattern. This is a good example of how difficult the analysis of RV data can be when searching for very low mass planets that induce low-amplitude signals lying close to the measurement precision. The results also point out the importance of following a star for a sufficiently long period of time until one can confidently secure the characterisation of the whole system, including the effects of stellar activity.

*Based on the work of Santos, Mortier, Faria, et al. 2014, A&A, 566, A35

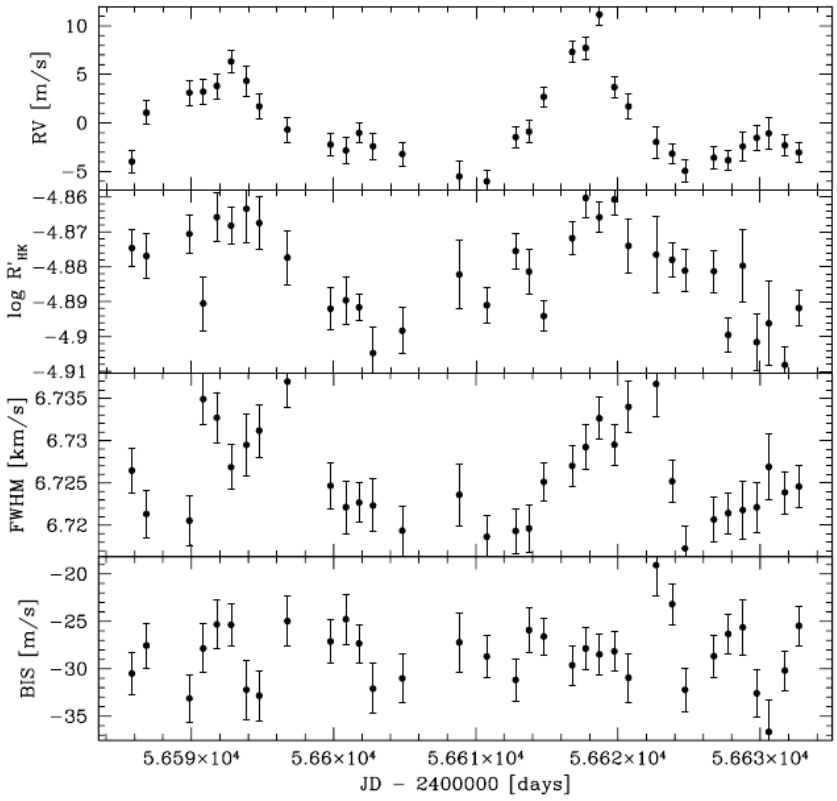

Figure 1: Time series of the radial velocity, stellar activity, FWHM, and BIS of HD 41248, for the period between JD = 2456580 and 2456640.

Complementary spectroscopic measurements using other wavelengths (e.g. near-IR) may be useful to distinguish real planets from activity-induced signals. A new generation of near-IR spectrographs is currently being developed which will open great perspectives in this domain.

References

[1] Santos, N. C., Mortier, A., Faria, J. P., et al. 2014, Astronomy and Astrophysics, 566, A35

[2] Gonzalez, G. 1997, Monthly Notices of the Royal Astronomical Society, 285, 403

[3] Santos, N. C., Israelian, G., & Mayor, M. 2001, Astronomy and Astrophysics, 373, 1019

[4] Sousa, S. G., Santos, N. C., Israelian, G., Mayor, M., & Udry, S. 2011, Astronomy and Astrophysics, 533, A141

[5] Mayor, M., Marmier, M., Lovis, C., et al. 2011, ArXiv e-prints

[6] Jenkins, J., Tuomi, M., Brasser, R., Ivanyuk, O., & Murgas, F. 2013, The Astrophysical Journal, 771, 41

A platform for LBL: a key to take properly into account the earth atmosphere transmittance

Giancarlo Pace 1[1]

[1]*Instituto de Astrofísica e Ciências do Espaço, Universidade do Porto, CAUP, Rua das Estrelas, PT4150-762 Porto, Portugal*

Abstract

The quest for rocky planets orbiting stars like the Sun poses difficult and exciting scientific and technological challenges, forcing us, sometimes, to improve on even well tested observational procedures. For instance, in the case velocity measurements from infra-red spectra, the level of accuracy mentioned above requires an unprecedently careful correction for telluric lines. The classical approach to correct for telluric lines is to observe a standard star along with the object. Standard stars are either hot stars, assumed to be featureless, or solar-stars, assumed to be known very precisely. One observes one such standard with the same instrumental set up and at the same airmass of the scientific target, just before or right after the actual observation of the target. For each observation of the standard, one then divides the observed spectrum for its synthetic counterpart, and obtains the spectrum of the terrestrial atmosphere transmission for that time and airmass, which is finally applied to the scientific observation of the target.

The method is a good one for the level of precision and accuracy typically required in most situations, but it has three limitations that need to be overcome in order to push further the limit of such precision. In the first place, it is very unlikely that a good reference star is observable at the same airmass, almost at the same time and with the same instrumental set up as the target. The ideal case would be to have reference star and scientific target the same field, but this does not happen very often. Consider also the loss of telescope time in any other case. The second limitation of the reference-star method is that it relies on assumptions which are not 100% realistic: hot stars are not featureless, solar stars are not perfectly known. In other words, the synthetic spectrum that we build for the reference star is not 100% accurate, thus also the accuracy of the spectrum of the earth-atmosphere transmission that is built upon it, is limited. Such limitation cannot be simply neglected if we want to detect small rocky planets orbiting distant stars. A solution would be launching a satellite with a very high-resolution spectrograph on board to build a catalogue of spectra with extremely high levels of signal-to-noise ratio, for a rich sample of reference stars well spread all over the sky. It is not difficult to convince the reader that this is not feasible and would have an extremely narrow scientific rationale. But it would also fail to overcome the last of the three limitation we are mentioning here, namely that the resolution of the telescope would blur out finer details of the interaction of the stellar light with the earth-atmosphere. As a matter of fact, the correction with a reference-star would be limited even if we had a perfect black body of the right brightness in the same field our target. In some specific cases, which is beyond our scope to discuss here, this circumstance would prevent us to achieve the precision we need to detect exo-earths, which we aim at.

The problems described above can be overcome by using accurate models of the earth atmosphere transmission. A very sophisticated code that allows us to do it: the LBLRTM (line by line

radiative transfer model). But the lack of clear instructions makes its use extremely challenging. That's why we are developing ULME, a user friendly platfom for the LBLRTM code. ULME means "the Use of the LBLRTM code Made Easy". You will find it soon on line.

The upper layers of Alpha-Centauri A: footprint of a new rapid variation layer

Ana Brito[1], Ilídio Lopes[1]

[1] *CENTRA, Pavilhão de Física, Piso 4, Instituto Superior Técnico, Lisboa, Portugal*

Abstract

Probing the structure of the upper layers of Sun-like stars is crucial to determine the physical mechanisms responsible for convection and magnetism in stars. In this work we use a nonlinear seismic diagnostic to infer the background structure responsible for the scattering of acoustic waves. By applying a seismic technique originally developed for the solar acoustic spectrum to the measurement of solar Helium abundance, from the acoustic oscillations of Alpha Centauri A we have discovered the existence of an unexpected glitch located 6% beneath the photosphere. Current theoretical stellar models do not predict this glitch. With the large amount of high quality asteroseismic data made available by COROT and Kepler missions, the use of this new technique can help to better understand the envelopes of solar type stars.

Fundamental stellar parameters determination for WTTS in NGC 2264

Ana C. S. Rei[1], Jorge F. Gameiro[1], Sílvia H. P. Alencar[2]

[1] *Centro de Astrofísica e Faculdade de Ciências da Universidade do Porto*
[2] *Universidade Federal de Minas Gerais*

Abstract

Low-mass (0.3 to 2 M$\odot$ (Petrov 2003)) young stellar objects, also known as T Tauri Stars (TTS), can be divided into two main groups: Classical T Tauri Stars (CTTS) and Weak-line T Tauri Stars (WTTS). CTTS show several photometric and spectroscopic features associated with chromospheric activity and accretion processes related with a circumstellar environment. One key feature of CTTS spectra is the presence of a *veiling* effect of photospheric lines due to an excess of continuum emission. On the other hand, WTTS spectral features are associated with chromospheric activity, and the presence of a non-accreting circumstellar disk. These pre-main-sequence (PMS) stars can be found in star forming regions, like NGC 2264. In order to study both activity and evolution of these stars one needs accurate determinations of stellar parameters, as the effective temperature (Teff) and the surface gravity (logg).

The spectra in study was obtained using VLT/FLAMES GIRAFFE spectrograph (R$\sim$17000) in the wavelength band: [6440-6815]Å. The usefullness of this band for the TTS lies on the presence of both the Hα line at 6562.8Å and the Li I line at 6707.7Å. The Hα line is an indicator for both chromospheric activity and accretion processes and the presence of Li I line is an indicator of youth (Soderblom 2010). On the other hand, this GIRAFFE band is not the most appropriated for stellar parameters determination, since it does not have many lines sensitive to both Teff and, specially, logg. The sample is composed by a total of 162 stars, each star have 20 spectra taken in several different nights from December 2011 and February 2012. 86 of those stars were classified as WTTS, according to the following criteria: the stars with EW(Hα)$\geq$10 Å and width at 10% Hα peak $\geq$ 200 Km/s are considered CTTS, otherwise they are classified as WTTS (Bertout 1989, Affer et al. 2013).

To perform the stellar parameters determinations for WTTS we used Spectroscopy Made Easy (SME) (Valenti et al. 1996). It is a spectral synthesis code generally used for high-resolution spectra but is also reliable at intermediate-resolution spectra. We defined 12 wavelength intervals containing mainly Fe, Ti and Ni lines that are not blended, avoiding the first part of the spectrum, that can be contaminated with telluric lines, the Li I line and the Hα line and its surroundings. After running some tests for the WTTS we decided discard the spectra with S/N$\leq$30 (reducing the sample to 45 WTTS). Also, the metallicity was fixed to the litterature value for the NGC 2264 cluster: [Fe/H]=-0.15 (Barry et al. 1979). The free parameters are Teff, logg and vsini. The method was validated for a sample of benchmark stars, for both high (HARPS) and intermediate (GIRAFFE) resolution spectra. The developed method to analyse GIRAFFE spectra can be used for both FGK main-sequence stars and pre-main-sequence WTTS. It allows the determination of stellar parameters in the band [6440-6815]Å for both high- and intermediate-resolution spectra. Since GIRAFFE is one of the spectrographs used in the context of the Gaia-ESO Survey, this method can be of great help for spectral analysis.

When we overplot the Siess PMS evolutionary tracks in a Teff vs logg diagram, we found that most of the stars are in the Henyey track with masses between TTS typical masses can range from 0.3 to 2 M⊙ (Petrov 2003). Some of the analyzed stars might be HAeBe stars (intermediate-mass PMS stars). For most cases the values of vsini range between 10 and 20 Km/s, typical values for WTTS, that rotate at around 10% the break up velocity (Bertout 1989).

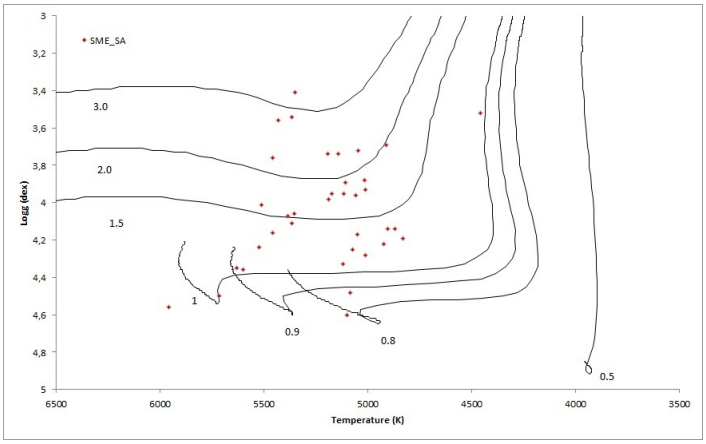

Figure 1: Effective temperature vs Logg diagram. The black lines represents the Siess evolutionary tracks for PMS stars (in solar masses). The red diamonds corresponds to the results for the WTTS present in the studied sample. The obtained results locates the WTTS between 1 and 2 M⊙, along the Henyey track.

According to the current paradigm, WTTS are the end of the PMS evolution and they are almost reaching the Main-Sequence, which is in agreement with our results.

Regarding future work, since the stars of the sample have been observed several time in a 2 month interval, we intend to study the spectroscopic variability of the Hα line, photospheric lines and Li I line for both CTTS and WTTS. We also intend to study the stellar activity of the CTTS (veiling, analysis of emission lines and measurements of accretion rates) and determinine mass and age for both CTTS and WTTS using MESA star code (Paxton et al. 2011).

References

[1] Affer, L., Micela, G., Favata, F., Flaccomio, E., Bouvier, J., MNRAS (2002)

[2] Barry, D.C., Cromwell, R.H. & Schoolman, S.A., ApJSS, Vol. 41, 119-130 (1979)

[3] Bertout, C., ARAA, Vol. 27:351-395 (1989)

[4] Paxton, B. et al., ApJ SS, 192:3 (2011)

[5] Petrov, P.P., Astrophysics, Vol. 46, N.4 (2003)

[6] Soderblom, D., ARAA (2010)

[7] Valenti, J.A. & Fischer, D.A., 159:141-166 (2005)

Impact of micro-telluric lines on precise radial velocities

Diana Cunha[1,2], N. C. Santos[1,2], P. Figueira[1], A. Santerne[3], J. L. Bertaux[2], C. Lovis[4]

[1] *Centro de Astrofísica da Universidade do Porto, Rua das Estrelas, 4150-762 Porto, Portugal*
[2] *Departamento de Física e Astronomia, Faculdade de Ciências, Universidade do Porto, Portugal*
[3] *Université Versailles Saint-Quentin; Sorbonne Université, UPMC Univ. Paris 06; CNRS/INSU, LATMOS-IPSL, 11 Boulevard d'Alembert, 78280 Guyancourt, France*
[4] *Observatoire Astronomique de l'Université de Genève, 51 Ch. des Maillettes, - Sauverny - CH1290, Versoix, Suisse*

Abstract

In a near future, new instruments such as ESPRESSO will arrive, allowing us to reach a precision in radial-velocity measurements of the order of ten cm/s. At this level of precision, several noise sources that until now have been outweighted by photon noise will start to contribute significantly to the error budget. The telluric lines that are not neglected by the masks for the radial velocity computation, here called micro-telluric lines, are one of such noise sources.

In this work we investigate the impact of micro-telluric lines in the radial velocities calculations. We also aim at investigating how to correct the effect of these atmospheric lines on radial velocities. The work presented here follows along two parallel lines. First, we calculate the impact of the micro-telluric lines by multiplying a synthetic solar-like stellar spectrum by synthetic atmospheric spectra and evaluate the effect created by the presence of the telluric lines. Then, we divide HARPS spectra by synthetic atmospheric spectra to correct for its presence on real data, and calculate the radial velocity of the corrected spectra. When doing so one considers two atmospheric models for the synthetic atmospheric spectra: the LBLRTM and TAPAS. We find that the micro-telluric lines can induce an impact in the radial velocities calculation that can be already of the order of the current precision achieved with HARPS, and so its effect should not be neglected, specially for future instruments such as ESPRESSO. Moreover, we find that the micro-telluric lines' impact depends on factors such as the radial velocity f the star, airmass, relative humidity, and the barycentric Earth radial velocity projected along the line of sight at the time of the observation.

Lithium Depletion on planet-host stars

P. Figueira[1], J. P. Faria[1,2], E. Delgado Mena[1], V. Zh. Adibekyan[1], S. G. Sousa[1,2], N. C. Santos[1,2], G. Israelian[3,4]

[1] *Centro de Astrofísica da Universidade do Porto, Rua das Estrelas, 4150-762 Porto, Portugal*
[2] *Departamento de Física e Astronomia, Faculdade de Ciências da Universidade do Porto, Portugal*
[3] *Instituto de Astrofísica de Canarias, 38200 La Laguna, Tenerife, Spain*
[4] *Departamento de Astrofísica, Universidad de La Laguna, 38206 La Laguna, Tenerife, Spain*

Abstract

It has been argued that planet-host stars show a Lithium abundance depletion when compared with their non-host counterparts (e.g. Gonzalez 2014, Delgado Mena et al. 2014). In this work we study the impact of the presence of planets on the lithium abundance of host stars, and evaluate the previous claim that planet hosts exhibit lithium depletion when compared to their non-host counterparts.

Using previously published lithium abundances from Delgado Mena et al. (2014), we remove the confounding effect of the different fundamental stellar parameters by applying a multivariable regression on our dataset. In doing so we make explicitly an assumption made implicitly by different authors: that lithium abundance depends linearly on fundamental stellar parameters. Using a moderator variable to distinguish stars with planets from those without, we evaluate the existence of an offset in lithium abundances between the two groups. We perform this analysis first for stars that present a clear lithium detection exclusively, and then including upper lithium measurements.

Our analysis shows that under the above-mentioned assumption of linearity, an offset in lithium abundance between planet hosts and non-hosts is recovered. This offset is negative, showing enhanced depletion for planetary hosts, and a statistically significant result (see Fig. **??**). By bootstrapping the error bars we concluded that an inflation on the lithium uncertainty estimations by a factor of larger than 5 is required in order to render the results non-significant. We demonstrated that the offset as delivered by our method depends on the different nature of the stars in the two samples. We did so by showing that if the planet-host stars are replaced by comparison stars in a mock planet-host sample, the offset is reduced down to zero. Moreover, the measured depletion is still significant when one imposes different constraints on the dataset such as a limit in planetary mass or constrain the host temperature to around solar value. We conclude then that planet-host stars exhibit enhanced lithium depletion when compared with non-host stars.

Acknowledgments

This work was supported by the European Research Council/European Community under the FP7 through Starting Grant agreement number 239953. PF and NCS acknowledge support by Fundação para a Ciência e a Tecnologia (FCT) through Investigador FCT contracts of reference IF/01037/2013 and IF/00169/2012, respectively, and POPH/FSE (EC) by FEDER funding through the program "Programa Operacional de Factores de Competitividade - COMPETE". EDM, SGS, and VZhA acknowledge the support from the Fundação para a Ciência e Tecnologia, FCT

(Portugal) in the form of the fellowships SFRH/BPD/76606/2011, SFRH/BPD/47611/2008, and SFRH/BPD/70574/2010 from the FCT (Portugal). GI acknowledges financial support from the Spanish Ministry project MINECO AYA2011-29060. PF and JF further thank the CrossValidated online community for enlightening discussions on statistical tests. We warmly thank all those who develop the *Python* language and its scientific packages and keep them alive and free.

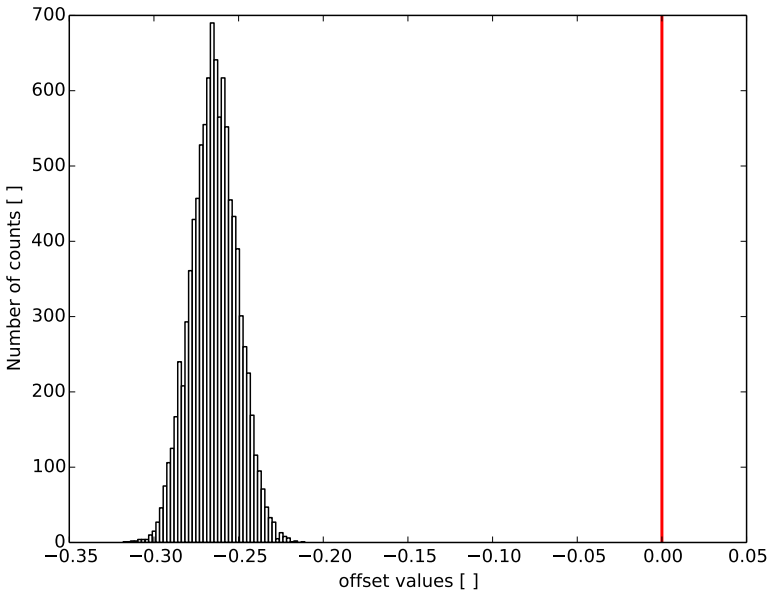

Figure 1: The distribution of offsets as obtained by bootstrapping the Li values around the respective error bars. The vertical red line represents the zero value for the offset.

References

[1] Gonzalez, G, MNRAS, 441, 1201 (2014)

[2] Delgado-Mena, E., Israelian, G., González Hernández, J. I., et al., A&A, 562A, 92 (2014)

Is there a signature of planet formation in solar analogs?

V. Zh. Adibekyan[1], J. I. González Hernández[2,3], E. Delgado Mena[1], S. G. Sousa[1,2,4], N. C. Santos[1,4], G. Israelian[2,3], P. Figueira[1], S. Bertran de Lis[2,3]

[1] *Centro de Astrofísica da Universidade do Porto, Rua das Estrelas, 4150-762 Porto, Portugal*
[2] *Instituto de Astrofísica de Canarias, 38200 La Laguna, Tenerife, Spain*
[3] *Departamento de Astrofísica, Universidad de La Laguna, 38206 La Laguna, Tenerife, Spain*
[4] *Departamento de Física e Astronomia, Faculdade de Ciências da Universidade do Porto, Portugal*

Abstract

After the first planets were discovered, astronomers have been trying to search for chemical signatures of planet formation on the planet-host stars. Several studies suggested that the chemical abundance trend with the condensation temperature, Tc, is a signature of terrestrial planet formation (e.g. Meléndez et al., 2009; Ramírez et al., 2009). In particular, that the Sun shows "peculiar" chemical abundances because of the presence of the terrestrial planets in our solar system (Meléndez et al., 2009). Although the interpretation of these findings has been strongly debated in other studies (e.g. González Hernández et al., 2010, 2013, hereafter GH10,13), the main reason of the observed chemical peculiarities was not identified.

Here we explore the origin of the trend observed between [X/H] (or [X/Fe]) and Tc using a sample of 58 solar analogs[1] from GH10,13. Fifteen out of 58 solar analogs in this sample are known to be host planets. The more detailed analysis and complete results are presented in Adibekyan et al. (2014).

After a detailed analysis, we found that the Tc trend strongly correlates with the surface gravity and stellar age (see Figure 1): old stars are more depleted in refractory elements (smaller refractory-to-volatile ratios) than their younger counterparts. At the same time we found no significant correlation between the Tc slope and other stellar parameters.

Since for G dwarf stars in the main sequence one does not expect significant changes in their atmospheric chemical abundances with age, we are led to believe that the observed correlation is likely to reflect the chemical evolution in the Galaxy.

Moving one step further, we found a tentative evidence that the Tc slopes correlate also with the mean galactocentric distance of the stars (R_{mean}), which we use as a proxy of the birth radii. This trend is indicating that stars which have originated in the inner Galaxy have less refractory elements relative to the volatiles.

Associating our findings with the planet formation, we showed that planet-hosting solar analogs are older (see Figure 1) and have smaller galactocentric distances, than their non-host counterparts. These results suggest that the difference in Tc slopes observed for solar analogs with and without planets is then probably due to the differences in their "birth places" and birth moment. Interestingly, Haywood (2009) has already shown that (giant) planet host stars tend to have smaller R_{mean} and probably originate in the inner disk, which point in the same direction as our findings.

Our findings lead us to two interesting conclusions i) The solar analogues with planets in the solar neighborhood mostly come from the inner Galaxy and ii) the age

[1] We defined solar analogs as stars with; T_{eff} = 5777±200 K; logg = 4.44±0.20 dex; [Fe/H] = 0.0±0.2 dex.

and galactic birth place are the main factors responsible for the abundance ratio of refractory to volatile elements in the stars.

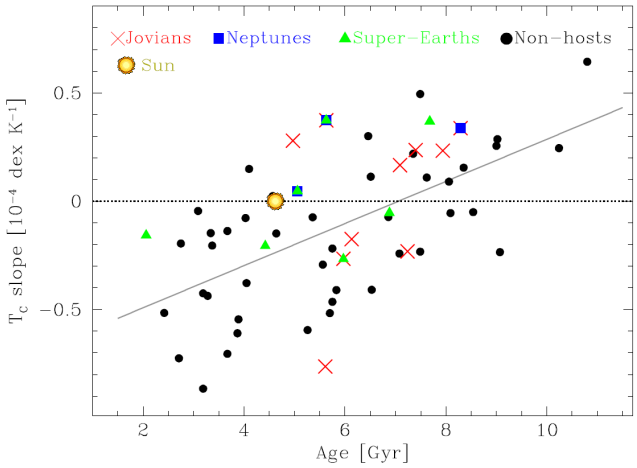

Figure 1: T_c slopes versus stellar ages for solar analog stars.

Acknowledgments

This work was supported by the European Research Council/European Community under the FP7 through Starting Grant agreement number 239953. V.Zh.A., S.G.S., and E.D.M are supported by grants SFRH/BPD/70574/2010, SFRH/BPD/47611/2008, and SFRH/BPD/76606/2011 from the FCT (Portugal), respectively. NCS also acknowledges support in the form of a Investigador FCT contract funded by FCT/MCTES (Portugal) and POPH/FSE (EC). G.I., S.B.L, and J.I.G.H. acknowledge financial support from the Spanish Ministry project MINECO AYA2011-29060, and J.I.G.H. also received support from the Spanish Ministry of Economy and Competitiveness (MINECO) under the 2011 Severo Ochoa Program MINECO SEV-2011-0187. PF is supported by the FCT and POPH/FSE (EC) through an Investigador FCT contract with application reference IF/01037/2013 and POPH/FSE (EC) by FEDER funding through the program "Programa Operacional de Factores de Competitividade - COMPETE.

References

[1] Adibekyan, V. Z., González Hernández, J. I., Delgado Mena, E., et al., A&A, 564, L15 (2014).

[2] González Hernández, J. I., Israelian, G., Santos, N. C., et al., ApJ, 720, 1592 (2010).

[3] González Hernández, J. I., Delgado-Mena, E., Sousa, S. G., et al., A&A, 552, A6 (2013).

[4] Haywood, M., ApJ, 698, L1 (2009).

[5] Meléndez, J., Asplund, M., Gustafsson, B., & Yong, D., ApJ, 704, L66 (2009).

[6] Ramírez, I., Meléndez, J., & Asplund, M., A&A, 508, L17 (2009).

The role of single-particle phase function on spectral deconvolution of asteroidal regoliths

M. A. Salgueiro Da Silva[1,2], Cristiana Silva[3], Teresa Seixas[1,2]

[1] *Departamento de Física e Astronomia da Faculdade de Ciências da Universidade do Porto*
[2] *Centro de Investigação da Terra e do Espaço da Universidade de Coimbra*
[3] *Departamento de Matemática da Faculdade de Ciências da Universidade do Porto*

Abstract

Hapke's radiative transfer theory provides a complete framework for modelling and deconvolution of reflectance spectra of minerals and intimate mixtures of minerals, as those forming asteroidal regoliths. According to Hapke's theory, however, the reflectance depends on a considerable number of a priori unknow parameters and wavelength-dependent variables, which may be specific to each mineral or mineral mixture. This is the case of the single-particle phase function that describes the angular distribution of reflected radiation by a single particle. Usually, it is assumed that the phase function depends only on the phase angle and that its symmetry parameters are characteristic of a given mineral. In this work, we show how the particle size dependence of the phase function predicted by Mie's theory can be used to improve the modelling and deconvolution of reflectance spectra of intimate mixtures of minerals.

Effect of stellar activity on the high precision transit light curve

Mahmoudreza Oshagh[1]

[1] *Centro de Astrofísica da Universidade do Porto, Portugal*

Abstract

Stellar activity features such as spots and plages can create difficulties in determining planetary parameters through spectroscopic and photometric observations. The overlap of a transiting planet and a stellar spot, for instance, can produce anomalies in the transit light curve that may lead to inaccurate estimation of the transit duration, depth, and timing. Such inaccuracies can affect the precise derivation of the planet's radius.

In this talk we will present the results of a quantitative study on the effects of stellar spots on high precision transit light curves. We show that spot anomalies can lead to the estimate of a planet radius that is 4% smaller than the real value. The effects on the transit duration can also be of the order of 4%, longer or shorter. Depending on the size and distribution of spots, anomalies can also produce transit timing variations with significant amplitudes. For instance, TTVs with signal amplitudes of 200 seconds can be produced by spots as large as the largest sunspot. Finally, we examine the impact of active regions on the transit depth measurements in different wavelengths, in order to probe the impact of this effect on transmission spectroscopy measurements. We show that significant (up to 10%) underestimation/overestimation of the planet-to-star radius ratio can be measured, especially in the short wavelength regime.

The stellar mass function of star-forming galaxies and the mass-dependent SFR function since $z = 2.23$

David Sobral[1,2]

[1] *Centro de Astronomia e Astrofísica da Universidade de Lisboa, Lisboa, Portugal*
[2] *Leiden Observatory, Leiden, The Netherlands*

Abstract

I will present the results from deep and wide narrow-band surveys undertaken with UKIRT, CFHT, Subaru and the VLT, a unique combined effort to select large, robust samples of (mostly) H-alpha (Ha) emitters at $z = 0.40$, 0.8, 0.84, 1.47 and 2.23 (corresponding to look-back times of 4.2, 7.0, 9.2 and 10.6 Gyrs) in a uniform manner over $2 - 10\,\mathrm{deg}^2$ in the COSMOS, UDS and SA22 fields. Our samples contain $1000 - 3000$ homogeneously selected Ha sources per redshift and are used to determine the Ha, star-formation rate and stellar mass functions (for star-forming galaxies) of the Universe and their 11 Gyr evolution. We unveil the strong exponential decline of the typical star formation rate of galaxies (SFR*) with time from z=2.23 to $z \sim 0$, at all masses, and very little evolution in the mass function of star-forming galaxies, consistent with them having a similar M* since $z \sim 2$. The stellar mass density within SFGs comprises $\sim 100\%$ of the stellar mass density in all galaxies at $z = 2.23$, and declines to $\sim 20\%$ by $z = 0.4$, driven by the rise of the passive population. We also show that there is no significant evolution in the fractional contribution from SFGs of different masses to the star formation rate density since $z = 2.23$ and that the decline of SFR* and of the star formation rate density are primarily driven by an exponential decline in SFRs at all masses. Our results have important implications on how SFGs need to be quenched across cosmic time, but also on the driver(s) of the exponential decline in SFR* since $z = 2.23$.

Hot-dust (690 K) Luminosity Density and Its Evolution in the Last 7.5 Gyr

Hugo Messiasl[1], Bahram Mobasher[2], José Manuel Afonso[1]

[1] *Centro de Astronomia e Astrofísica da Universidade de Lisboa, Portugal*
[2] *University of California Riverside, United States of America*

Abstract

We study the contribution of hot-dust to the luminosity density of galaxies and its evolution with cosmic time. Using the Spitzer-IRAC data over an area of $1.8\,\mathrm{deg}^2$ covered by the Cosmic Evolution Survey (COSMOS) field, we estimate the contribution from hot-dust at rest-frame $4.2\,\mu$m (from $0 \lesssim z \lesssim 0.2$ up to $0.5 \lesssim z \lesssim 0.9$). This wavelength corresponds to blackbody temperature of $\sim 690\,\mathrm{K}$. The contribution of stellar emission is estimated from the rest-frame $1.6\,\mu$m luminosity (assumed to result from stellar emission alone) and subtracted from the mid-infrared luminosity of galaxies to measure hot-dust emission. To attempt the study of the $3.3\,\mu$m polycyclic aromatic hydrocarbon (PAH) feature, we use the rest-frame $4.2\,\mu$m to infer the hot-dust flux at $3.3\,\mu$m.

This study is performed for different spectral types of galaxies: early-type, late-type, starburst, and IR-selected active galactic nuclei (AGNs). We find that (1) the decrease of the hot-dust luminosity density since $0.5 \lesssim z \lesssim 1$ is steeper (by at least $0.2\,\mathrm{dex}$) compared with that of the cold-dust, giving support to the scenario where galaxy obscuration increases with redshift, as proposed in the literature; (2) hot-dust and PAH emission evolution seems to be correlated with stellar mass, where rest-frame $1.6\,\mu$m luminous non-AGN galaxies (i.e., massive systems) show a stronger decrement (with decreasing redshift) in hot-dust and PAH emission than the less luminous (less massive) non-AGN galaxies; (3) despite comprising $\lesssim 3\%$ of the total sample, AGN contribute as much as a third to the hot-dust luminosity density at $z < 1$ and clearly dominate the bright-end of the total hot-dust luminosity density function at $0.5 \lesssim z \lesssim 0.9$; (4) the average dust-to-total luminosity ratio increases with redshift, while PAH-to-total luminosity ratio remains fairly constant; (5) at $M_{1.6} > -25AB$, the dust-to-total and PAH-to-total luminosity ratios increase with decreasing luminosity, but deeper data are required to confirm this result.

Future study is necessary to further enlighten the characterization of the different spectral components at play in $2 - 5\,\mu$m spectral regime.

Extreme CII emission in type 2 quasars at z 2.5: a signature of kappa-distributed electron energies?

Andrew Humphrey[1]

[1] *Centro de Astrofísica da Universidade do Porto, Portugal*

Abstract

We have investigated the flux ratio between the 1335 A and 2326 A lines of singly ionized carbon in the extended narrow line regions of type 2 quasars at $z \sim 2.5$. We find the observed [CII 1335] / [CII 2326] flux ratio, which is not sensitive to the C/H abundance ratio, to be often several times higher than predicted by the canonical AGN photoionization models that use solar metallicity and a Maxwell-Boltzmann electron energy distribution. We have studied several potential solutions for this discrepancy: low gas metallicity, shock ionization, continuum fluorescence, and kappa-distributed electron energies. Although we cannot definitively distinguish between several of the proposed solutions, we argue that a kappa distribution gives the more natural explanation. We also present a new grid of AGN photoionization models using kappa-distributed electron energies.

Evaluating the robustness of state-of-the-art Spectral Synthesis codes when applied to Active Galaxies

Leandro Machado Cardoso[1], Jean Michel Gomes[1], Polychronis Papaderos[1]

[1] *Centro de Astrofísica and Faculdade de Ciências, Universidade do Porto, Rua das Estrelas, 4150-762 Porto, Portugal*

Abstract

Aim. Quantify the robustness of state-of-the-art Semi-empirical Population Synthesis codes in retrieving the star formation history and other relevant stellar population quantities (e.g. stellar mass, mean age and mean metallicity) of active galaxies.

Methods. Synthetic optical spectra of active galaxies were computed with our Evolutionary Population Synthesis code REBETIKO using solar Bruzual & Charlot (2003) Single Stellar Populations (SSPs) and a toy AGN model parameterised by a power-law, $F(\nu) \propto \nu^{-\alpha}$. These fictitious active galaxies were modelled using STARLIGHT (Cid Fernandes et al. 2005) with a library of SSPs comprising 25 ages and 4 metallicities (Z = 0.2, 0.4, 1 and 2.5 $Z_{\odot}$).

Results. The stellar mass as inferred by STARLIGHT suffers an overestimation with decreasing model age and increasing AGN power and α, reaching maximum values between 1 and 3 dex for 0.2 and 0.8 AGN relative flux contributions at $\lambda_0 = 4020$ Å, respectively. On one hand, the retrieved mean stellar age at AGN power of 0.8 can be over or underestimated by a factor between ∼1.3 and ∼0.8 if the model is young ($Age <$ 100 Myr) or old ($Age >$ 1 Gyr), respectively. This trend is minimised with decreasing AGN power. On the other hand, the recovered mean stellar metallicity can be overestimated by factors between ∼1.1. and ∼1.4 when the AGN power increases from 0.2 to 0.8. This overestimation however decreases with increasing α.

Introduction

We produced fictitious galaxy spectra over the full optical wavelength range using the evolutionary population synthesis code REBETIKO, created by Gomes & Papaderos. This code combines Simple Stellar Populations (SSPs) while considering different star formation rate and chemical evolution functions. Purely-stellar galaxy models covering all main galaxy evolutionary stages were created using SSPs from Bruzual & Charlot (2003) with solar metallicity.

It was added to these synthetic purely-stellar galaxy models a *toy AGN model* parameterised by $F_\nu \propto \nu^{-\alpha}$ (e.g. Koski 1978) and described by two parameters: (i) power-law index α, which serves as a proxy to the AGN continuum hardness, with α = 0.5, 1.0, 1.5 and 1.8, and (ii) relative AGN contribution at $\lambda_0 = 4020$ Å, tracing the AGN power at λ_0 for AGN_{power} = 0.2, 0.4, 0.6 and 0.8.

Modelling & Conclusions

We used STARLIGHT (Cid Fernandes et al. 2005) with a SSP library comprising 25 ages and 4 metallicities (Z = 0.2, 0.4, 1 and 2.5 $Z_{\odot}$) to retrieve information on the stellar populations of our active galaxy models. Figure 1 shows results for an $AGN_{power} = 0.4$ and instantaneous initial SFH.

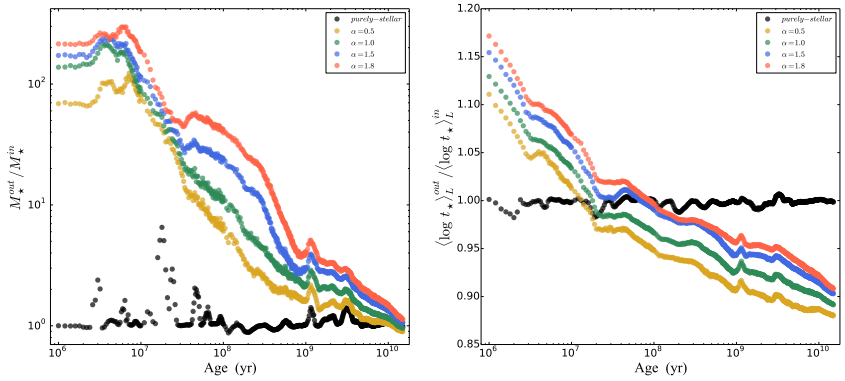

Figure 1: Variation of the ratio between output (STARLIGHT results for the active galaxy models) and input (purely stellar REBETIKO models) of the *stellar mass* $M_\star$ (*left panel*) and *mean stellar age weighted by light* $\langle \log t_\star \rangle_L$ (*right panel*) with model age, for an AGN relative contribution of 0.4 at $\lambda_0 = 4020$ Å. The black, yellow, green, blue and red circles correspond to purely-stellar and $\alpha = 0.5$, 1.0, 1.5 and 1.8 active galaxy models, respectively.

The *left panel* shows the ratio between the estimation made using STARLIGHT of the *stellar mass* $M_\star$ divided by the value for the corresponding purely-stellar REBETIKO model as a function of model age. This plot shows an increasing stellar mass overestimation with decreasing model age when an AGN is introduced. This overestimation increases with increasing α (i.e. flattening of the AGN continuum) and AGN power. Indeed, overestimations of a factor between 1 and 3 orders of magnitude is found when the AGN power increases from 0.2 to 0.8.

The *right panel* shows the *mean age of the stellar population weighted by light* $\langle \log t_\star \rangle_L$ as a function of model age. The mean age is overestimated if the model is young (Age $<$ 100 Myr) and underestimated if it is old (Age $>$ 1 Gyr). The over and underestimations factors reach maximum values of $\sim$1.3 and $\sim$ 0.8, respectively, when the AGN power is 0.8. Moreover, there is a consistent overestimation of the mean stellar age with increasing α.

STARLIGHT also shows an increasing overestimation of the *mean stellar metallicity weighted by light* $\log\langle Z_\star \rangle_L$ with AGN power, raising from a maximum factor of $\sim$1.1 up to $\sim$1.4 when the AGN power increases from 0.2 to 0.8. In contrast to the estimation of the stellar mass and mean stellar age, however, the mean stellar metallicity decreases with increasing α.

These results suggest that non-negligible over/underestimations of key stellar population properties of active galaxies might plague state-of-the-art Spectral Synthesis codes such as STARLIGHT. These biases seem correlated with the AGN continuum hardness and power, here represented by the power-law slope α and the AGN relative contribution, respectively.

References

[1] Bruzual, G.; Charlot, S., MNRAS, 344, 1000 (2003).

[2] Cid Fernandes, R., A. Mateus, L. Sodré, G. Stasinska, and J. M. Gomes, MNRAS, 358, 363 (2005).

[3] Koski, A. T., ApJ, 223, 56 (1978).

Herschel-ATLAS and ALMA: HATLASJ142935.3-002836, a major merger at z=1.027?

Hugo Messiasl[1], Rob Ivison[2], H-Atlas Team[3]

[1] *Centro de Astronomia e Astrofísica da Universidade de Lisboa, Portugal*
[2] *European Southern Observatory, Germany*
[3] *H-ATLAS, Germany*

Abstract

CONTEXT: The galaxy population appearing bright at sub-millimetre wavelengths is believed to comprise, among local galaxies and radio-loud sources, intrinsically active star-forming galaxies and gravitationally lensed (GL) sources. The latter provides an opportunity to pursue a study at a detail level beyond that enabled by the observation facility.

AIMS: This work focus on one of those lensed system candidates, HATLASJ142935.3-002836 (H1429-0028), selected via the Negrello et al.(2010) criterion in the Herschel-ATLAS field. Gathering a rich multi-wavelength data-set, we aim to confirm the scenario and model the background source's morphology and dynamics, as well as to pursue a full physical characterisation of it.

METHODS: Multi-wavelength high-resolution data (including ALMA Cycle-0) is utilised to assess the nature of the system. A lensing-analysis algorithm which fits simultaneously different wavebands is adopted to characterise the lens. The background galaxy dynamical information is studied by reconstructing the source-plane of the ALMA CO(4-3) transition data-cube. HST and Keck-AO imaging is used to constrain rest-frame optical photometry independently for the fore and background systems. Physical parameters (such as stellar and dust masses) are estimated via modelling of the spectral energy distribution (SED) taking into account source blending, foreground obscuration, and differential magnification.

RESULTS: The system is comprised of a foreground edge-on disc galaxy (at $z_{\rm sp} = 0.218$) and an almost complete Einstein ring around it, with possibly a quad-lens morphology. The background source is at $z_{\rm sp} = 1.027$ and is magnified by a factor of 8-10 depending on wavelength. It is comprised by two components (one dominating at rest-frame optical wavelengths, the other at FIR-to-radio wavelengths) and a 10's kpc-long tidal tail resembling the Antennae merger. It is a massive system ($1.32^{+0.63}_{-0.41} \times 10^{11}\,{\rm M}_\odot$) forming stars at a rate of $394^{+91}_{-88}\,{\rm M}_\odot\,{\rm yr}^{-1}$, and has a significant gas reservoir $M_{\rm ISM} = 4.6 \pm 1.7 \times 10^{10}\,{\rm M}_\odot$ (comprising 26^{+15}_{-13}% of the baryonic mass). Its depletion time due to star formation alone is thus expected to be $\tau_{\rm SF} = M_{\rm ISM}/SFR = 117 \pm 51\,{\rm Myr}$. The dynamical mass is estimated to be $5.8 \pm 1.7 \times 10^{10}\,{\rm M}_\odot$, and, together with the photometric total mass estimate, it implies that H1429-0028 is a candidate for a major merger system ($1 : 2.8^{+1.8}_{-1.5}$). The comparison between the millimetre and radio range yields no strong evidence for active galactic nucleus activity.

Evolution of the fine-structure constant in runaway dilaton models

Pauline Vielzeuf[1], Carlos Martins[1]

[1] *Centro de Astrofsica da Universidade do Porto, Portugal*

Abstract

We study the detailed evolution of the fine-structure constant α in the string-inspired runaway dilaton class of models of Damour, Piazza and Veneziano. We provide constraints on this scenario using the most recent observational datasets and discuss ways to distinguish these models from alternative models for varying α.

We find that in the range of model parameters which saturate bounds from current observations the redshift drift signal differs significantly from that of the canonical CDM paradigm. Measurements of this signal by the forthcoming European Extremely Large Telescope (E-ELT) will thus dramatically constrain these scenarios.

ESERO Portugal

Cátia Cardoso[1], Ana Noronha[1]

[1] *Ciência Viva*

Abstract

ESERO (European Space Education Resource Office) is an educational project of the European Space Agency (ESA) that uses space as an inspiring channel to teach Science, Technology, Engineering and Mathematics (STEM).

The ESERO main objectives are to:

· Motivate and enable young people to enhance their literacy and competence in sciences and technology (STEM disciplines).

· Inspire and enable young people to consider pursuing a career in the STEM field, in the space domain in particular.

· Contribute to increase youngsters' awareness of the importance of ESA and space research, exploration and applications in modern society and economy.

The ESERO project is developed in collaboration with national institutions with links to science education. There are currently 8 national ESERO offices in Europe.

In Portugal, the project was developed with Ciência Viva, formalizing an already existent collaboration between the two entities. ESERO Portugal has its headquarters in Pavilhão do Conhecimento – Ciência Viva, in Lisbon and at national level it collaborates directly with 5 Ciência Viva Science Centres: Centro Ciência Viva de Vila do Conde, Centro Ciência Viva de Aveiro – Fábrica, Centro Ciência Viva de Coimbra – Exploratório, Centro Ciência Viva do Lousal and Centro Ciência Viva de Sintra.

One of the aims of ESERO Portugal is to develop and adapt resources to the Portuguese curricula and train teachers. It does that by promoting teacher training courses, developing new classroom resources and adapting existing ones that correspond to the Portuguese teachers' needs. ESERO Portugal is also creating an online based repository of resources that can be used in the classroom. The first teacher training workshop organized by ESERO Portugal at national level had the participation of almost 100 teachers. These numbers reveal the large interest that teachers have for this thematic. The resources designed by ESERO Portugal want to empower teachers to discuss science themes with more confidence in the classroom.

ESERO Portugal also promotes scientific and technological competitions for students like CanSat and Zero Robotics. These projects want to provide a first contact of the students with the space industry reality. The students have to develop a full project for a specific scientific mission with a list of constraints and limitations, just like they would have to for a real project. The competitions

are challenging at the scientific and technological level, but they also are intent to develop the students' soft skills. Some of the Portuguese students that participated in these competitions at the secondary level followed scientific undergraduate degrees after and they stated that this experience was one of the deciding factors in their career options.

ESERO Portugal is working with the national community of scientists and engineers to promote synergies between the educational and research communities, to adapt space resources to the curricula and inspire students. ESERO Portugal invites scientists and engineers to participate and collaborate in the activities developed. ESERO Portugal is also working on a section of their webpage to help increase the visibility of the Portuguese Space industry and research with lower level teachers and students. The objective is to provide information about the universities and industry and their projects to give insight in the space area.

Figure 1 shows some examples of the activities developed by ESERO Portugal. These projects have inspired the creation of new projects and brought new experiences and ideas to the participants. This type of interactions and exchanges enrich the students, the teachers and the Portuguese educational system.

Acknoledgements: C.Cardoso thanks the Fundação para a Ciência e Tecnologia (FCT), Portugal for the Grant SFRH/BGCT/52550/2014.

Figure 1: Some examples of the activities that ESERO Portugal organizes: CanSat, MissionX, Teacher Training Courses.

Olympiads of Astronomy 2014 edition

Alexandre Aibéo[1,2,3], Jorge Grave[1,4] and Manuel Silva[5].

[1] *Centro de Astrofísica da Universidade do Porto, Rua das Estrelas, 4150-762 Porto, Portugal*
[2] *Escola Superior de Tecnologia e Gestão de Viseu, Campus Politécnico, 3504-510 Viseu*
[3] *Sociedade Portuguesa de Astronomia*
[4] *Universidade Lusófona do Porto, Rua Augusto Rosa, nº 24, 4000-098 Porto.* [5] *SIM and Faculdade de Ciências da Universidade de Lisboa, Edifício C8, Campo Grande, 1749-016 Lisboa, Portugal;*

Abstract

The Olympiads of Astronomy is a cornerstone of SPA's visible face in popular dissemination of astronomy. In such particular case, the target is high school students.

It is a competition organized by SPA with the fundamental help and dedication of its members who generously give time to create the tests, correct them, participate actively in the public program during the national final's event and also to coach the national team.

For the past few years, two major goals have been outlined: to increase the number of candidates and to increase the national representation at the international astronomy Olympiads.

Resuming the work done in previous editions, this year the national final took place in Coimbra, a region where there are, traditionally, a small number of candidates, thus intending to promote the competition's visibility. Moreover, three most important measures were taken, targeting to increase the number of candidates: to enable schools to form lists of candidates with five plus two extra elements; to increase the focus of promotion of the competition for girls and also on 10th grade students. Both these two fractions of the candidates have been decreasing in the last years. Such actions made a small but significant difference in the overall numbers: the number of candidates increased 20%, one third of the total number were girls and 40% of it were 10^{th} grade students. The impact was also felt in the ten selected elements to compete in the national final: one of them was a 10thgrade student and two of them were girls. Such conjunction was a very first for the last years of competition.

The SPA members as well as the ENAA participants had the opportunity to meet the team and wish them good luck. SPA is an open community that is also worried in nurturing the next generation of astronomers.

This year, a major financial effort was made to gather a team of four elements to represent Portugal in the international competition in Suceava, Romania. It was the first time the team was composed of four elements (three boys and a girl), a number of elements still lower to the common teams from other countries. Our "dream team" was trained by two members of the SPA for two weeks with a strong focus on both theoretical and observational practices.

All the effort and commitment of the team, the trainers and the organization was rewarded with the best performance ever: two honourable mentions for Diogo Cruz, from Domingos Sequeira Secondary School, Leiria and Marta Maria Eduarda, from Secondary School Infanta D. Maria, Coimbra. It is an important result, especially regarding the bases laid for an even better performance in future international competitions.and the impact on the promotion of astronomy in the younger public.

And Now for Something Completely Different

Distinguished participants[1]

[1] *Planet Earth, Solar System, Orion Arm, Milky Way galaxy, The Local Group, Virgo Supercluster*

Figure 1: From left to right: José Afonso, Carlos Martins, Nuno Gomes, Narsireddy Anugu.

Figure 2: Left: António Amorim presenting GRAVITY. Also in the picture (from left to right) Manuel Silva, André Moitinho (back), Ilídio Lopes and Paulo Garcia (back). Center: Marco Pinto. Right: José Pedro Vieira.

Figure 3: Left: Inês Leite. Center: Jorge Rocha (session chair) and Miguel Ferreira (speaker). Right: Ana Catarina Leite.

Figure 4: Top left: Alberto Krone-Martins (where is his mind?), Manuel Silva and Eduardo Alves. Top right: Carlos Correia (left) and Narsireddy Anugu. Bottom: André Moitinho, António Amorim, Ana Mourão, plus some others reading email or rushing to the coffee-break.

Figure 5: Left: Angela Santos, Leandro Cardoso, João Faria and Henrique Messias. Right: From left to right: André Moitinho, Dário Passos, Carlos Martins, João Pedro Vieira, Cátia Cardoso (far in the back), Giancarlo Pace (occulted), Maximilian von Wietersheim-Kramsta, Ana Marta Pinho, Ana Catarina Leite, Rui Alves, Leandro Cardoso (back) and Alexandre Aibéo (enjoying a most exquisite orange cocktail).

Figure 6: Left: João Pedro Vieira goes for the fruit, Cátia Cardoso smiles, Maximilian von Wietersheim-Kramsta, Giancarlo Pace, Carlos Correia (at far back), Ana Marta Pinho, Rui Alves, Mar Pino Charlez, Ângela Santos (far back), Alexandre Aibéo talks to Nuno Gomes, Miguel Ferreira (front). Center: Masato Minamitsuji explains his poster to Jorge Rocha. Right: Marco Pinto points a detail in the instrument configuration.

Figure 7: Left: Inês Leite reading the posters. Centre: Nelma Silva, Alberto Krone-Martins, Manuel Silva and José Afonso. Right: Eduardo Alves

Figure 8: From left to right: Pedro Leal, Rui Alves, Ana Marta Pinho and Masato Minamitsuji.

Figure 9: From left to right: Dário Passos, Ângela Santos and João Faria.

Figure 10: From left to right: Giancarlo Pace, Ana Brito, Ana Rei and Sandra Costa.

Figure 11: Left: Alberto Krone-Martins. Right: Nuno Gomes (back), Alexandre Aibéo, Cátia Cardoso (oculted), Carlos Martins (with aura), Rui Alves, Ana Marta Pinho, Ana Catarina Leite (oculted), Mar Pino Charlez (oculted) and Maximilian von Wietersheim-Kramsta.

Figure 12: From left to right: Sandra Costa, Paulo Garcia, Masato Minamitsuji, Ilídio Lopes (turned back), João Fernandes (turned back) and André Moitinho.

Figure 13: Left: from left to right: Pedro Figueira, Mahmoudreza Oshagh, Vardan Adibekyan (oculted) and David Sobral. Center: Diana Cunha. Right: Pedro Figueira.

Figure 14: From left to right: Vardan Adibekyan, Salgueiro da Silva, Mahmoudreza Oshagh.

Figure 15: From left to right: David Sobral, Andrew Humphrey and Leandro Cardoso.

Figure 16: From left to right: Hugo Messias, Pauline Vielzeuf and Cátia Cardoso.

Figure 17: From left ro right: Dário Passos and Alexandre Aibéo.

Figure 18: Presentation of two the Portuguese National Astronomy Olympics Winners by the organizers. From left to right: Manuel Silva, Maria Eduarda Marta (winner), Pedro Ribeiro (winner), Alexandre Aibéo and Jorge Grave.

Figure 19: Presentation of the Portuguese National Astronomy Olympics Winners.

Figure 20: Left: Cátia Cardoso, Dário Passos (oculted) and Patrícia Gonçalves. Right: UP TV journalist interviewing Paulo Garcia.

Figure 21: From left to right: Jorge Grave, Manuel Silva and Narsiredy Anugu.

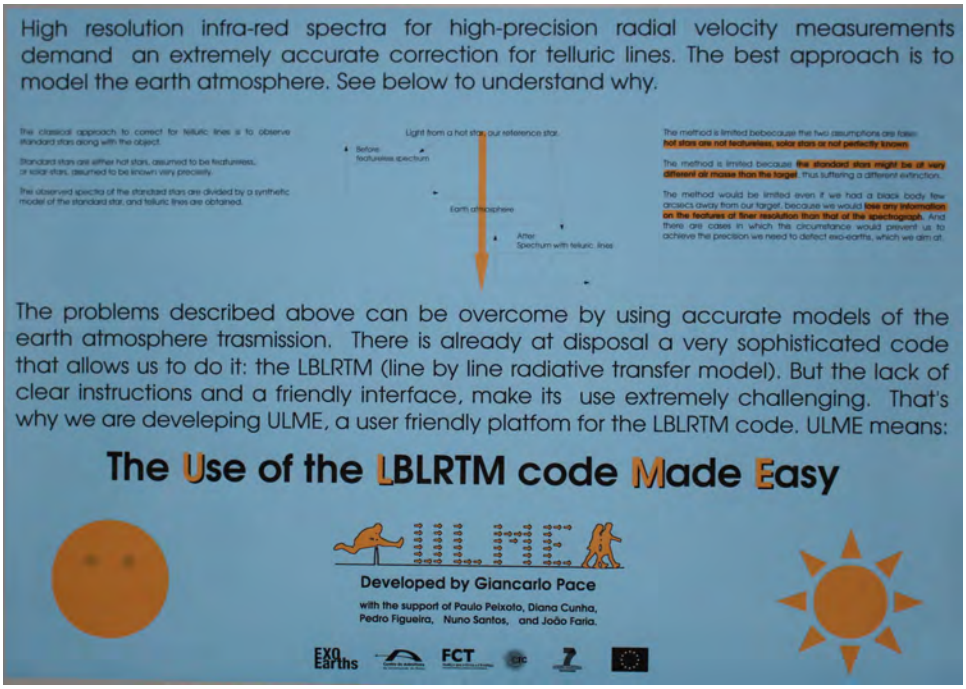

Figure 22: The most original poster in ENAA.

List of Authors

Abreu, Jorge, 7, 9, 11, 13
Adibekyan, Vardan, 53
Afonso, José, 1
Afonso, José Manuel, 61
Aibéo, Alexandre, 73
Alencar, Sílvia, 47
Alves, Eduardo P., 27
Alves, Rui, 31, 33
Amorim, António, 7, 9, 11, 13
Anugu, Narsireddy, 7, 9, 11, 13
Avelino, Pedro, 39

Bertaux, J. L., 49
Bertran de Lix, S., 53
Blind, Nicolas, 11, 13
Brito, Ana, 45
Burtscher, Leonard, 13

Cardoso, Cátia, 71
Cardoso, Leandro, 65
Charbonneau, Paul, 37
Correia, José, 21
Cunha, Diana, 49
Cunha, Margarida, 39

da Silva, M. A. Salgueiro, 55
da Silva, Rui, 17
Delplancke, Françoise, 15

Eisenhauer, Frank, 7, 11, 13

Faria, João, 41
Ferreira, Miguel, 23
Figueira, Pedro, 51, 53
Fonseca, Ricardo, 27
Frigola, Oriol, 23

Gameiro, Jorge, 47
Garcia, Paulo, 5, 7, 9, 11, 13
Gomes, Jean Michel, 65
Gomes, Nuno, 5, 15
Gordo, Paulo, 7, 9, 11, 13
Grave, Jorge, 73
Grismayer, Thomas, 27

Hernández, J. I. González, 53
Humphrey, Andrew, 63

Israelian, G., 53
Ivison, Rob, 67

Leal, Pedro, 29
Leite, Ana Catarina, 25
Leite, Inês, 21
Lopes, Ilídio, 45
Lovis, C., 49

Martins, Carlos, 3, 21, 23, 25, 29, 31, 33, 69
Mena, E. Delgado, 53
Messias, Hugo, 1, 61, 67
Minamitsuji, Masato, 35
Mobasher, Bahram, 61
Monteiro, Mafalda, 23

Oshagh, Mahmoudreza, 57
Ott, Thomas, 13

Pace, Giancarlo, 43
Papaderos, Polychronis, 65
Passos, Dário, 37
Pedrosa, P., 25
Pfhul, Oliver, 11
Pinho, Ana Maria, 31, 33

Rei, Ana, 47

Santerne, A., 49
Santos, Ângela, 39
Santos, Nuno C., 49, 53
Seixas, Teresa, 55
Silva, Cristiana, 55
Silva, Luís, 27
Silva, Manuel, 73
Sobral, David, 59
Solà, Joan, 23
Sousa, Sérgio G., 53

Team, H-Atlas, 67
Thiébaut, Éric, 5

Ventura, Luís, 29
Vieira, José Pedro, 19
Vielzeuf, Pauline, 69

Wieprecht, Ekkehard, 13